



NEW APPROACH TO STRONG EARTHQUAKE PREDICTION IN THE SOUTH BAIKAL REGION ON THE BASIS OF ROCK DEFORMATION MONITORING DATA: METHODOLOGY AND RESULTS

S.A. Bornyakov ¹✉, A.I. Miroshnichenko ¹, G.V. Vstovsky², A.E. Sintsov³, D.V. Salko¹

¹Institute of the Earth's Crust, Siberian Branch of the Russian Academy of Sciences, 128 Lermontov St, Irkutsk 664033, Russia

²CJSC Melnikov Central Research and Design Institute of Construction Metal Structures, 49 Architect Vlasov St, Moscow 117997, Russia

³JSC Foreign Trade Organization "Security", 34A Taganskaya St, Moscow, 109147, Russia

ABSTRACT. The Southern Baikal is located within the actively developing Baikal rift zone (BRZ) that is characterized by a significant seismic potential, and $M > 7$ earthquakes occur periodically with intensive shaking in the epicenters (up to 10 units). The problem of prediction and forecasting of strong earthquakes has always been critical for this region, considering its increasing urbanization, industrial clusters and transport systems. The article describes the methodology based on rock deformation monitoring data, which aims at developing a technology capable of efficient prediction and forecasting of strong earthquakes. In the Institute of Earth's Crust SB RAS a set of studies is carried out in order to solve this problem, including those associated with the instrumental study of current movements of the lithosphere through GPS geodesy and deformations of rocks by strain gauges. The existing GPS sites and deformation measurements are combined into the Large-Scale Research Facilities "South Baikal instrumental complex for monitoring hazardous geodynamic processes" in frame of the Shared Research Facilities "Geodynamics and Geochronology" at the Institute of the Earth's Crust, Siberian Branch of the Russian Academy of Science.

In this article, the deformation monitoring methodology is described in application to the monitoring sites installed in the study area. The description includes the details of its conceptual basis, technical support and data processing methods. The discussion focuses on the instrumental measurements of rock deformation related to three strong events in the study area – Kultuk (August 27, 2008), Bystrinskoe (September 21, 2020), and Kudara (December 10, 2020) earthquakes. The features of the deformation process before these seismic events are given special attention with account of the structural-geodynamic settings and positions of local monitoring sites relative to the earthquake epicenters.

KEYWORDS: rock deformation monitoring; earthquake; precursor; prediction

FUNDING: The study was carried out under financial support provided by the Russian Foundation for Basic Research (project 21-55-53019). This work involved the Large-Scale Research Facilities "South Baikal instrumental complex for monitoring hazardous geodynamic processes" in frame of the Shared Research Facilities "Geodynamics and Geochronology" at the Institute of the Earth's Crust SB RAS.

RESEARCH ARTICLE

Received: December 8, 2021

Revised: January 18, 2022

Accepted: January 20, 2022

Correspondence: Sergey A. Bornyakov, bornyak@crust.irk.ru

FOR CITATION: Bornyakov S.A., Miroshnichenko A.I., Vstovsky G.V., Sintsov A.E., Salko D.V., 2022. New Approach to Strong Earthquake Prediction in the South Baikal Region on the Basis of Rock Deformation Monitoring Data: Methodology and Results. *Geodynamics & Tectonophysics* 13 (2), 0588. doi:10.5800/GT-2022-13-2-0588

НОВЫЙ ПОДХОД К ПРОГНОЗУ СИЛЬНЫХ ЗЕМЛЕТРЯСЕНИЙ В ЮЖНО-БАЙКАЛЬСКОМ РЕГИОНЕ НА ОСНОВЕ ДАННЫХ МОНИТОРИНГА ДЕФОРМАЦИИ ГОРНЫХ ПОРОД: МЕТОДОЛОГИЯ И РЕЗУЛЬТАТЫ

С.А. Борняков¹, А.И. Мирошниченко¹, Г.В. Встовский², А.Е. Синцов³, Д.В. Салко¹

¹ Институт земной коры СО РАН, 664033, Иркутск, ул. Лермонтова, 128, Россия

² ЗАО «ЦНИИПСК им. Мельникова», 117997, Москва, ул. Архитектора Власова, 49, Россия

³ АО ВО «Безопасность», 109147, Москва, ул. Таганская, 34А, Россия

АННОТАЦИЯ. Южное Прибайкалье (ЮП) находится в пределах активно развивающейся Байкальской рифтовой зоны (БРЗ), обладающей значительным сейсмическим потенциалом. Здесь периодически происходят землетрясения с магнитудой более 7 и с интенсивностью сотрясений в эпицентрах до 10 баллов. В условиях высокой степени урбанизации ЮП и активного развития в его пределах промышленных кластеров и транспортных систем существенно повышается актуальность проблемы прогноза сильных землетрясений. В ИЗК СО РАН для решения этой проблемы проводится комплекс исследований по разным направлениям. Одно из них связано с инструментальным изучением современных движений литосферы на больших базах посредством GPS-геодезии и деформаций горных пород на малых базах штанговыми тензометрическими датчиками. Существующие пункты GPS и деформационных измерений объединены в уникальную научную установку «Южно-Байкальский инструментальный комплекс для мониторинга опасных геодинамических процессов» (УНУ «ЮБИК»), входящую в состав ЦКП «Геодинамика и геохронология».

В статье рассмотрены методические вопросы деформационного мониторинга на малых базах. Описаны его концептуальная основа, техническая база и методы обработки получаемого фактического материала. На примере произошедших в последнее время в ЮП трех сильных землетрясений – Култукского (27.08.2008 г.), Быстринского (21.09.2020 г.) и Кударинского (10.12.2020 г.) – показаны предшествующие им особенности развития деформаций горных пород, а также влияние на них структурно-геодинамических условий в местах расположения пунктов мониторинга и пространственного положения этих пунктов относительно готовящегося очага землетрясения.

КЛЮЧЕВЫЕ СЛОВА: мониторинг деформаций горных пород; землетрясение; предвестник; прогноз

ФИНАНСИРОВАНИЕ: Исследование выполнено при финансовой поддержке РФФИ (проект № 21-55-53019) с использованием УНУ «Южно-Байкальский инструментальный комплекс для мониторинга опасных геодинамических процессов», входящей в состав ЦКП «Геодинамика и геохронология» Института земной коры СО РАН.

1. INTRODUCTION

The Southern Baikal region (Russian: Pribaikalie) is the southern part of East Siberia near Lake Baikal. It is located within the actively developing Baikal rift zone (BRZ) that is characterized by a significant seismic potential. Minor seismic events are frequent in this region, and $M > 7$ earthquakes occur periodically with intensive shaking in the epicenters (up to 10 units). The problem of prediction and forecasting of strong earthquakes has always been critical for this region, considering its increasing urbanization, industrial clusters and transport systems. The search for solutions to this problem is carried out in different directions, including instrumental monitoring of rock deformation on local sites.

In 1987, the first measurements of rock deformation in the study area were taken by a laser strain meter installed by the Institute of Laser Physics SB RAS in an adit near the Talaya Seismic Station (Baikal Branch of Geophysical Service SB RAS). The Institute team was focused on searching for earthquake precursors. The long-term monitoring records taken in 1987–2015 showed that horizontal deformations in the study area were related to sublatitudinal

displacements of crustal blocks at a rate of 1–10 mm/yr; and long-term variations in crustal deformation were caused by the stress accumulation and release during strong earthquakes. Based on this data, a phenomenon of oscillation excitation in a range of 0.3–10 seconds was discovered for the first time in relation to the deformation process [Timofeev et al., 1994; Timofeev, 2004; Fomin et al., 2019].

In the 1990s, a monitoring site was installed in a local fault outcrop near the observatory of the Institute of Solar-Terrestrial Physics SB RAS in the village of Listvyanka, Irkutsk region. This facility is used for experimental studies aimed at developing a technology for controlling the displacement regime in active fault zones. Numerous experiments have shown that high stresses in the upper part of such faults can be safely released by controlled technogenic impacts that trigger weak seismogenic motions along the faults [Psakhie et al., 2001, 2004; Ruzhich et al., 2002, 2007, 2020].

In 2008, the SDVIG recorder was installed in the adit near the Talaya Seismic Station [Ruzhich, 2004]. This hardware system consolidates the rock deformation monitoring database that is used to substantiate theoretical and

methodological principles for developing a new approach to intermediate- and short-term prediction and forecasting of earthquakes [Bornyakov, Vstovsky, 2010; Vstovsky, Bornyakov, 2010].

Local detailed rock deformation monitoring is currently performed by a network of monitoring sites installed in the study area in 2012 [Salko, Bornyakov, 2014]. Deformation signals are recorded by modern gauges and sensors and analyzed to identify the features and details of the deformation process before strong earthquakes, which can be considered as earthquake precursors. The deformation monitoring site at the Talaya Seismic Station has been recently reequipped, and three new monitoring sites were installed on the NW coast of Lake Baikal. The network of these sites is a part of the South Baikal instrumental complex for monitoring hazardous geodynamic processes provided by the Centre for Geodynamics and Geochronology at the Institute of the Earth's Crust, Siberian Branch of the Russian Academy of Sciences.

In this article, we discuss the perspectives of rock deformation monitoring through consideration of the technology capable of efficient earthquake prediction and forecasting. The rock deformation monitoring methodology is described in application to the monitoring sites in the study area. The description includes the details of its conceptual basis, technical support and data processing methods. The discussion focuses on the instrumental measurements of rock deformation signals directly related to three strong events in the study area – Kultuk (August 27, 2008; $M=6.3$), Bystrinskoe (September 21, 2020; $M=5.4$), and Kudara (December 10, 2020; $M=5.5$) earthquakes. Here, we describe the signs of an upcoming earthquake, which are detectable as the features of the deformation process and can be considered as earthquake precursors.

2. BASIC CONCEPTS FOR ELABORATING A TECHNOLOGY USING ROCK DEFORMATION DATA FOR SHORT-TERM PREDICTION OF EARTHQUAKES

A framework for elaborating a technology for forecasting a tectonic earthquake or any other currently understudied natural phenomenon must include a theoretical model that adequately describes this natural phenomenon. Furthermore, prognostic indicators based on this model should be continuously detectable. Modern studies of tectonic earthquake sources are mostly based on the concept of avalanche-unstable fracturing (AUF) [Myachkin, 1978] and the stick-slip model [Brace, Byerlee, 1966]. The AUF model describes the way the numerous small ruptures occur and grow, merging rapidly and forming a long fault later on, i.e., the process which causes seismogenic displacement along the fault. In contrast, the stick-slip model describes the process of periodic seismogenic activation of an existing fault.

In the investigations of large active continental lithospheric faults, the stick-slip mechanism is observed to occur more often than the unstable fracturing and thus given more attention in studies aimed at earthquake prediction. In the 1960–1990 s, the researchers performed numerous laboratory experiments using the stick-slip model to investigate and assess the recurrence of seismogenic displacements on faults. Physical phenomena preceding the displacements were recorded and analyzed in order to identify possible precursors of earthquakes. In combination with the findings from theoretical studies and field observations, the results of these experiments have significantly improved the understanding of the earthquake source physics and made it possible to offer a wide range of short-term precursors [Cicerone et al., 2009]. Anomalous behavior of geophysical parameters before an earthquake was considered

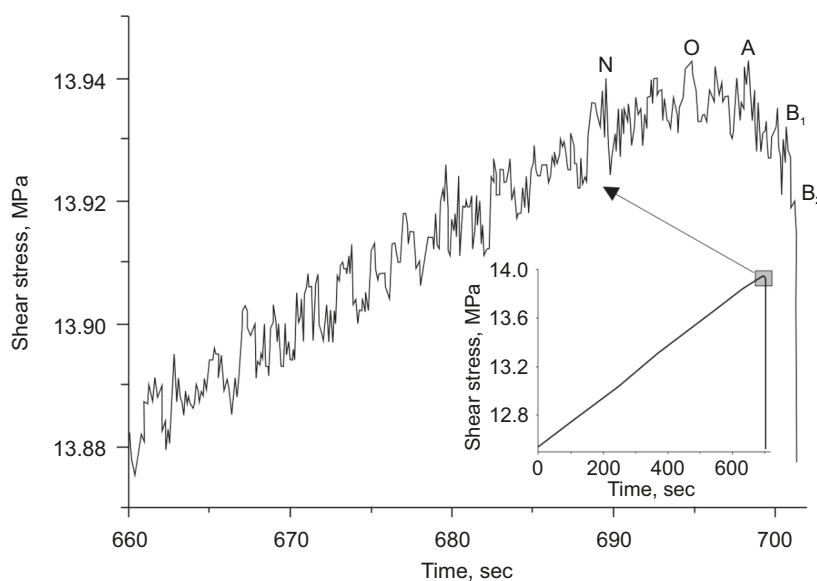


Fig. 1. Shear stress vs time before the slip impulse (after [Ma et al., 2014]). Inset (right corner) – linear graph of the shear stress increase; the slip impulse is marked by a grey box.

Рис. 1. График изменения сдвигового напряжения во времени перед импульсной подвижкой (малый график справа) и его увеличенный фрагмент в критической точке, показанный маленьким серым квадратом (по [Ma et al., 2014]).

as a precursor. However, many of these studies were based on outdated concepts and thus failed to solve the problem of earthquake prediction and forecasting. Furthermore, their results raised doubts whether seismic forecasting is ever possible [Geller et al., 1997]. Some progress has been achieved by using the concept of synergetics [Haken, 1978, 1983; Prigogine, Kondepudi, 2002]. In this context, a seismically active fault can be considered as an open nonequilibrium dynamic system; an earthquake is a self-organized criticality (SOC) [Bak, Tang, 1989]; and a "coherent" behavior is typical of the deformation process just before an earthquake [Feder H.J.S., Feder J., 1991; Ciliberto, Laroche, 1994; Olami et al., 1992].

The SOC model has been confirmed in experiments using a precision servo-controlled press to simulate seismic activation of faults due to the stick-slip mechanism [Ma et al., 2012, 2014]. According to these results, in a loaded system of two blocks contacting along a rupture, the deformation process preceding the occurrence of a slip impulse develops in stages.

These stages are marked by changes in the average shear stress over time (Fig. 1). The graph shows shear stress variations and illustrates the deformation dynamics of the entire boundary between the interacting blocks before the occurrence of the slip impulse (marked by a grey box at an interval of 660–700 sec, see the inset in Fig. 1). In segment N–O, the graph deviates from linearity. At point O, the shear stress reaches its maximum value, and the system goes to the metastable state. In segment OAB₂, the meta-instability state is achieved. It includes the early (AB₁) and late (B₁B₂) meta-instability substages. After point B₂, dynamic instability manifests itself as a slip impulse. At the first metastable stage, relative displacements of the blocks start and develop along with slow relaxation of the stresses accumulated at the interblock contact. This process takes place in the quasi-creep stationary mode, which is caused by the occurrence of small micro-sources of destruction (i.e. small activated segments of the rupture). During the early meta-instability substage, the stress continues to decrease slowly, and the isolated segments of the rupture continue to increase gradually. The late meta-instability substage is characterized by accelerated synergism – the deformation becomes intensified and accelerated. The synergism manifests itself immediately before the transformation of the quasi-static state into a dynamic one due to the coherent behavior of all activated segments, which implies their

self-organization. In a natural setting, it is reasonable to expect that the meta-instable stage of the activation of a fault can be detected by self-organization of its segments.

Thus, the stick-slip model in its synergistic interpretation [Ma et al., 2012, 2014] demonstrates that the critical dynamic state of a fault / fault zone (which is achieved at the late meta-instability substage) should be investigated in detail as a potential earthquake precursor rather than an anomalous variation of any geophysical parameter of the fault / fault zone. A direct and evidence-based indicator of the critical dynamic state (i.e. the meta-instability substage) is self-organization of activated fault segments at the fault plane immediately before seismogenic rupturing of the certain fault. Considering natural faults, we suggest that the self-organization process can be diagnosed by a digital analysis of the time series of rock deformation signals. We have tested this research approach by spectral analysis [Scargle, 1982, 1989; Savransky, 2004; Bornyakov et al., 2017], entropy analysis [Brillouin, 1966; Zubarev et al., 2002; Bornyakov, 2008], and fractal analysis [Mandelbrot, 1982; Velde et al., 1990], and the structural functions curvature analysis method (SFCAM) [Vstovsky, 2006, 2008; Bornyakov, Vstovsky, 2010].

3. ROCK DEFORMATION MEASUREMENT ON LOCAL SITES

In our study, a database of rock deformation measurements is consolidated by an original instrumental complex (IC) [Salko, Bornyakov, 2014]. The IC includes a data collection-transmission unit (DCTD), analog-to-digital converters (ADC), analog bar-shaped sensors, an autonomous power supply system (APSS), a remote base server, and client-server control software packages (Fig. 2). The IC is designed to receive rock deformation signals, take their accurate time-related measurements, compile a flash-memory dataset, and transfer the datasets to the remote base server via the on-line mobile communication system.

The DCTD unit uses a RS485 bus for simultaneous connection of up to 32 ADCs. The number of sensors used is determined by the number of ADC channels. In one- and two-channel designs, 32 and 64 sensors can be connected to the channels, respectively. Measurements are taken by bar-shaped sensors calibrated to meter linear deformation. The ADC polls the sensors with a discreteness of 8 Hz/10 seconds, calculates the average of the accumulated 80 values, and sends the average value to the DCTD unit. These data are

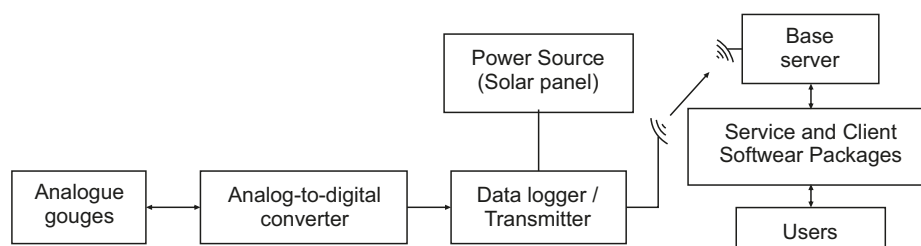


Fig. 2. Block diagram of the instrumental complex designed for rock deformation monitoring.

Рис. 2. Блок-схема инструментального комплекса для мониторинга геофизических параметров.

then transmitted and input to the server database, and thus, a time series data is obtained every 10 seconds.

The IC collects the data from four monitoring sites located on the southern and southwestern shores of Lake Baikal (Fig. 3, a). The Talaya, Listvyanka, Buguldeika, and Olkhon monitoring sites are described below.

4. DESCRIPTION OF THE ROCK DEFORMATION MONITORING SITES

The Talaya site is located on the southern shore of Lake Baikal (Fig. 3, a, b). It includes 10 bar sensors installed in an abandoned adit that is characterized by constant temperature and humidity (Fig. 4). A bar sensor structure includes

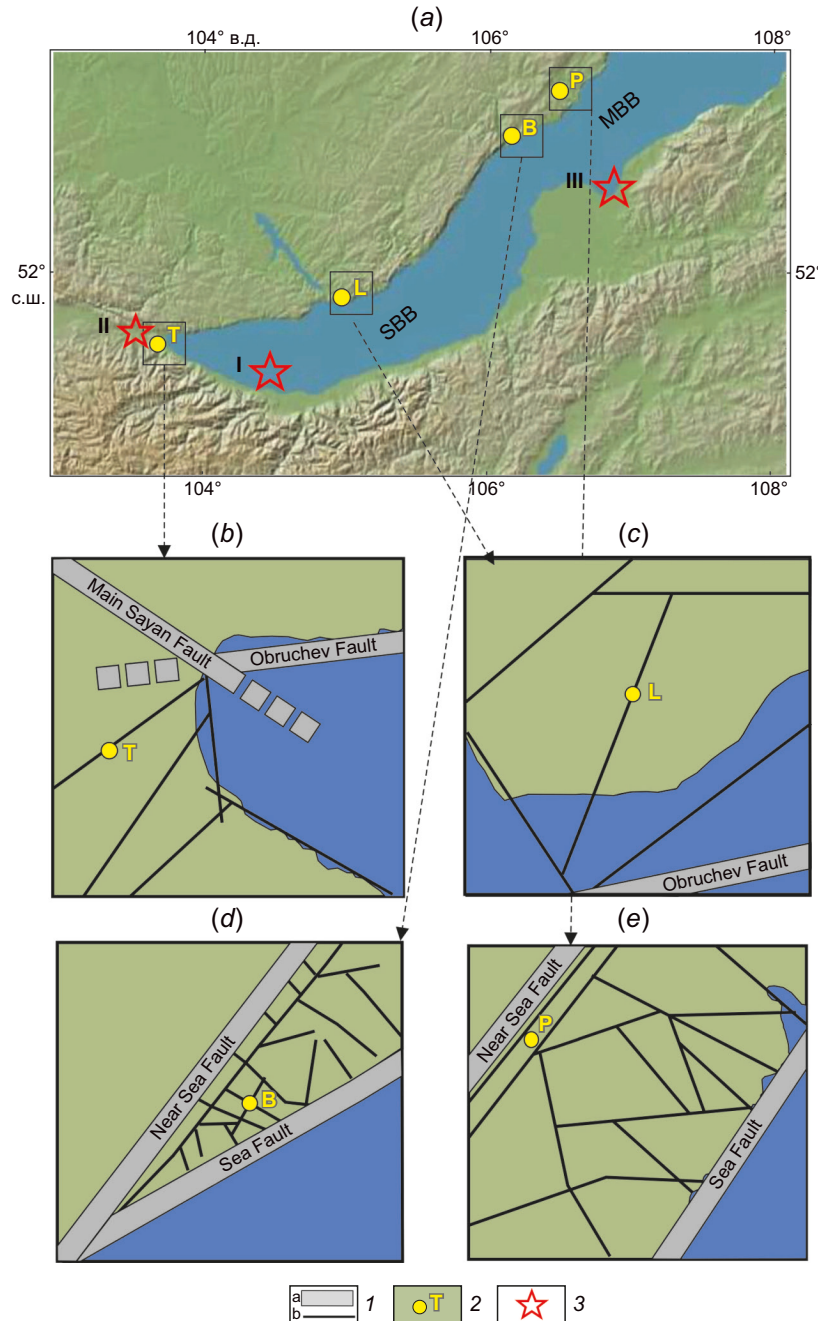


Fig. 3. Locations of the rock deformation monitoring sites in the Southern Baikal region (a), and their structural-geodynamic settings (b-e).

1 - major (a) and minor (b) local faults; 2 - monitoring sites: T - Talaya, L - Listvyanka, B - Buguldeika, P - Olkhon; 3 - earthquake epicenters: Kultuk (I), Bystrinskoe (II), Kudara (III); MBB - South Baikal basin; SBB - Middle Baikal basin.

Рис. 3. Места расположения (a), структурные и геодинамические условия (b-e) в окрестности пунктов деформационного мониторинга в Южном Прибайкалье.

1 - крупные структурообразующие (a) и второстепенные, локальные (b) разломы; 2 - пункты мониторинга: Т - «Талая», L - «Листвянка», В - «Бугульдейка», Р - «Приольхонье»; 3 - эпицентры Култукского (I), Быстринского (II) и Кударинского (III) землетрясений; МВВ - Южно-Байкальская и SBB - Среднебайкальская впадины.

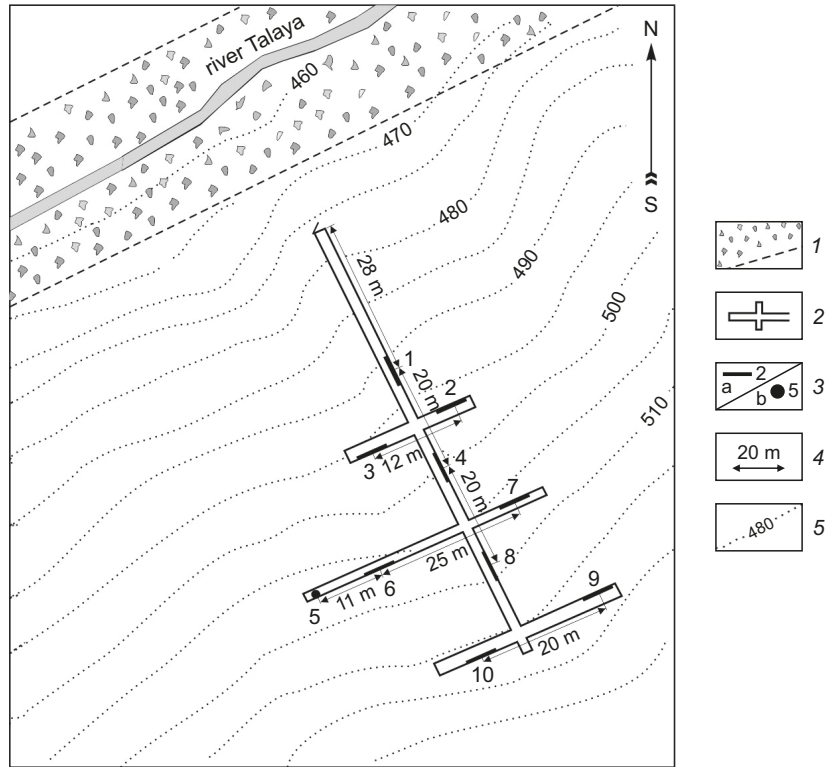


Fig. 4. A sketch of the network of sensors installed in the adit (Talaya site).
 1 - fault zone; 2 - adit contours; 3 - bar sensors in horizontal (a) and vertical (b) positions, and their numbers (1-10); 4 - distance between bar sensors; 5 - topography lines and heights relative to the sea level.

Рис. 4. Пространственная сеть штанговых датчиков в штольне пункта «Талая».
 1 - зона разлома; 2 - контуры штольни; 3 - штанговые датчики, расположенные горизонтально (а), вертикально (б) и их номера (1-10); 4 - расстояния между датчиками; 5 - изолинии рельефа с указанием высоты относительно уровня моря.

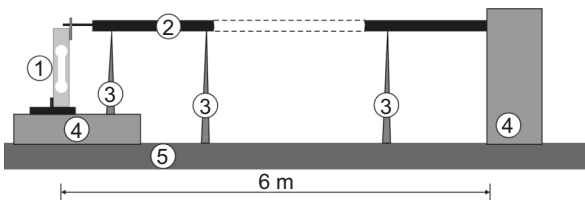


Fig. 5. Schematics of the bar sensor installation in the adit. See the text for explanations.

Рис. 5. Схема установки штангового датчика в штольне. Пояснения в тексте.

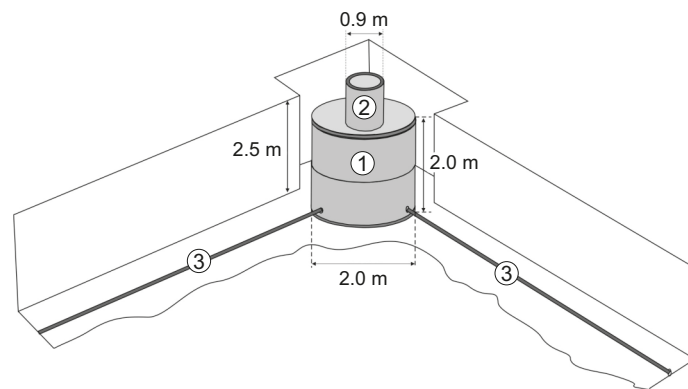


Fig. 6. Schematics of the Buguldeika rock deformation monitoring site.
 1 - round-shaped chamber made of two pre-cast reinforced concrete rings (each 0.9 m high and 2.0 m in diameter); 2 - pre-cast concrete pipe (0.9 m in diameter) and used as an access into the chamber from the ground surface; 3 - 10 m long bar sensor.

Рис. 6. Схема устройства пункта деформационного мониторинга «Бугульдейка».
 1 - бокс из двух железобетонных колец (высотой 0.9 м и диаметром 2 м); 2 - железобетонное кольцо диаметром 0.9 м используемое для спуска в бокс с поверхности земли; 3 - штанговые датчики.

a strain gauge (1), steel bar (square cross-section, total length of 6.0 m) (2), and mobile supports (3) preventing any sidewise or vertical displacement of the bar sensor (Fig. 5). One end of the bar is fixed into a concrete pedestal (4) that is rigidly connected with the rock (5). Its other end is connected to a strain gauge installed on the same concrete pedestal (Fig. 5). Throughout the year, the air temperature in the adit remains rather stable which excludes any influence of the temperature factor on rock deformation measurements.

At the Listvyanka, Buguldeika and Olkhon monitoring sites on the southwestern shores of Lake Baikal, the sensors are installed in underground bunkers in order to minimize the influence of the temperature factor. Constructed at depths of 2.5–3.0 m, the bunkers differ in length and width and range in height from 1.8 to 2.0 m. Each bunker is covered with a one-meter thick soil layer. At the Listvyanka site, the bar sensor (10 m long) is installed in a vertical drill hole in the bunker, and rock deformation measurements are made. At the Buguldeika site, two horizontally installed bar sensors (each 10 m long) take measurements in two orthogonal directions (Fig. 6). One sensor is oriented to the south-east – this position takes into account the regional crustal extension of the Baikal rift zone (BRZ), which is caused by the movement of the Transbaikalia block to the south-east. The Olkhon site includes two spatially separated "sub-sites". One sub-site is constructed similarly to the Listvyanka site, and has a vertical bar sensor (12 m long). The second sub-site is located at a distance of 140 meters south-east of the first one. Its structure is similar to that of the Buguldeika site (Fig. 6), except that it has one horizontal SE-oriented sensor (10 m long) to monitor the regional crustal extension of BRZ.

5. STRUCTURAL-GEODYNAMIC SETTINGS OF THE MONITORING SITE LOCATIONS

The monitoring sites are located in different structural-geodynamic settings. The Talaya site is located on the shore at the southern termination of Lake Baikal. Its geodynamic setting is dominated by the right flank of a local fault zone that cuts the Talaya river valley (see Fig. 3, a, b). This is the area of conjugation of the major structure-forming faults, Main Sayan and Obruchev. It should be noted that the geodynamics of the lithosphere in the Southern Baikal region is determined by the compression from the Hindustan collision area, and the compression setting here transforms into the SE-trending extension, as confirmed by the regional studies [Sankov et al., 2014].

The Listvyanka site is installed in a local fault zone in the coastal block bordered by the Obruchev fault (see Fig. 3, c). The crystalline basement of the South Baikal basin has subsided along the fault to a depth of more than 8.0 km and is covered by a 6.0 km thick layer of non-lithified and weakly lithified sedimentary deposits [Logachev, 1999]. This layer hinders propagation of the SE-trending extension from the Transbaikalia area to the coastal block, although the consolidated basement of the South Baikal basin transmits the deformation effect the lower part of the

block. Thus, the Listvyanka site records the rock deformation that occurs as an indirect response of the local fault zone to the deformation processes in the lower part of the coastal block.

The Buguldeika site is located at the junction zone of two local faults in a wedge-shaped crustal block between the zones of the Primorsky and Morskoy faults (see Fig. 3, d). Its geodynamic setting is similar to that of the Listvyanka site. The only difference lies in a shallow waterdepth of the Baikal on the Buguldeika-Selenga link between the South and Middle Baikal basins (35–400m) [Bukharov, 1996] (see Fig. 3, d). Currently, the regional SE-trending extension is transmitted to the lower horizons of the wedge-shaped block (this situation is similar to that of the Listvyanka site). In comparison to the block monitored by the Listvyanka site, this block has a smaller cross-section. Furthermore, wide weak fault zones are observed at the frontal and rear parts of the block. Due to these factors, it is involved into "swinging" oscillatory movements in the regional extension direction (i.e. SE-trending).

The Olkhon site is located 14 km away from the Lake Baikal shore, outside the area of dynamic influence of the Morskoy fault zone characterized by a large vertical displacement amplitude (see Fig. 3, e). As described above, the rock deformation measurements are taken at the two sub-sites installed at a distance of 140 meters from each other and in different structural settings, i.e. one in the local fault zone, and the other within the undisturbed crustal block.

6. ROCK DEFORMATION DATA ANALYSIS

6.1. The main components of rock deformation

The analysis of the time series of rock deformation measurements shows that deformation takes place as an oscillatory process, and oscillation periods vary widely both in time and size [Bornyakov et al., 2016, 2017]. It is possible to distinguish two groups of deformation components which appeared due to external and internal factors (in relation to the Earth). Respectively, such components are termed external and internal. The external factors are lunar and solar tides and variations in atmospheric pressure. The tides can cause variations in deformation amplitudes every 12 or 24 hours (Fig. 7, a, b). In the study area, 12-hour deformation variation cycles are clearly observed only at the Talaya site and modulated into two-week cycles (Fig. 7, a, c). The tidal deformation amplitudes range from a few microns to a few dozen microns, depending on the positions of the Earth, the Moon and the Sun relative to each other.

The deformation response of rocks to atmospheric pressure variations is of a selective nature and manifests itself most clearly in case of a sharp pressure increase. In rock deformation monitoring records, it is detectable as a deformation pulse with amplitude from a few microns to a few dozen microns (Fig. 8). When atmospheric pressure changes gradually or drops sharply, the deformation response is either weak or absent.

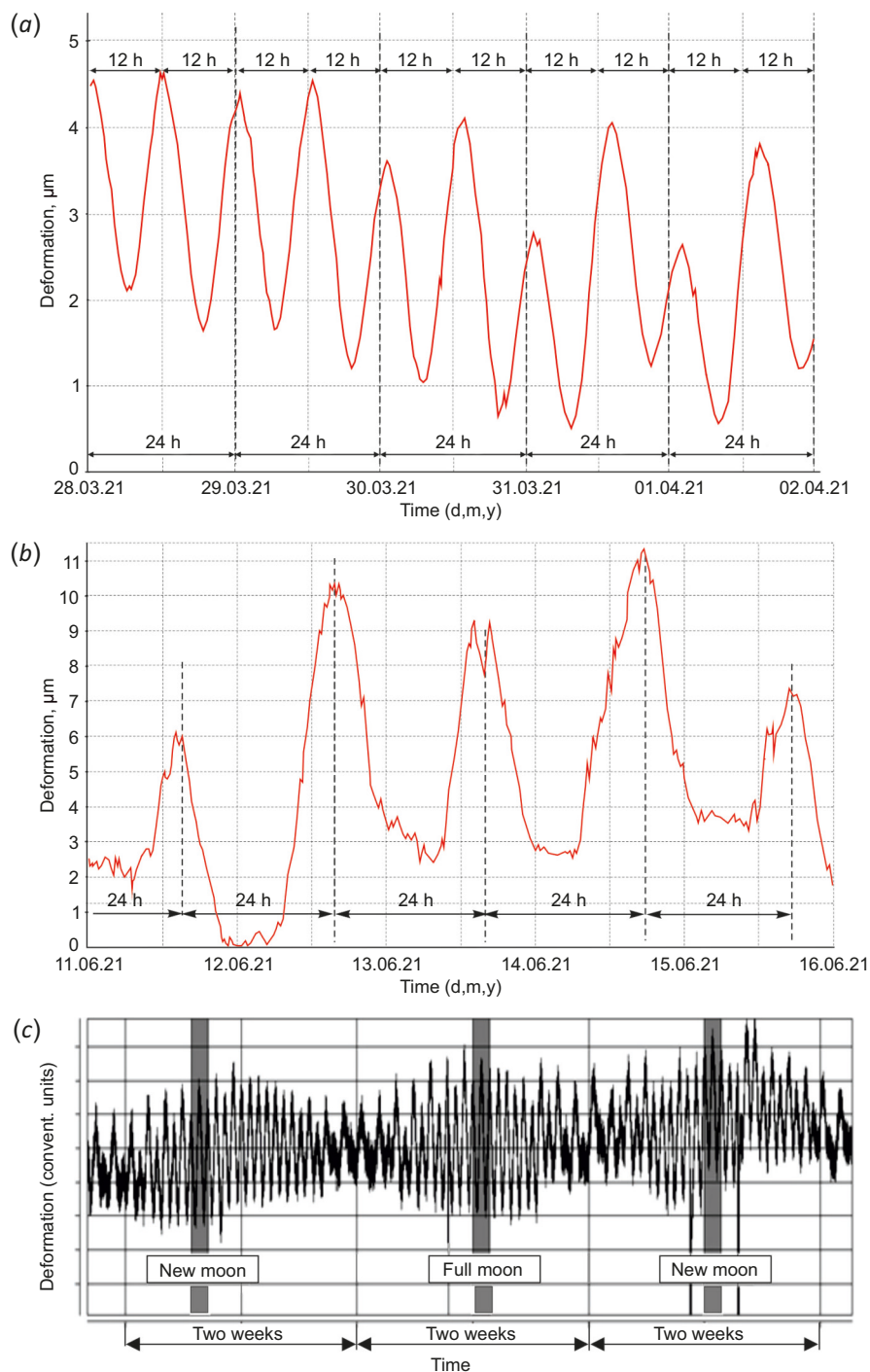


Fig. 7. The 12- (a) and 24-hour (b) variations in the rock deformation due to lunar and solar tides, and two-week modulations of 12-hour variations (c) in Talaya site.

Рис. 7. Двенадцати- (a) и двадцатичетырехчасовые (b) вариации деформаций, обусловленные лунно-солнечными приливами, и двухнедельные модуляции двенадцатичасовых вариаций (c) в пункте «Талая».

In the group of deformation components appeared due to internal factors of a tectonic origin, we distinguish non-periodic and periodic deformations, i.e. temporary and permanent, respectively [Bornyakov et al., 2019].

Non-periodic deformation is observed as a single pulse that vary in shape and amplitude (Fig. 9), whose sporadic occurrence is monitored and recorded as a single deformation wave. Spatial migration velocities of such waves

vary from a few centimeters to a few dozen centimeters per second.

In general, two types of the non-periodic deformation waves are distinguished by differences in their main parameters. In the rock deformation time series, Type 1 is detected as an asymmetric pulse with an amplitude of a few dozen microns (Fig. 9, a), which is recorded by several closely spaced monitoring sites and, as a rule, accompanied by

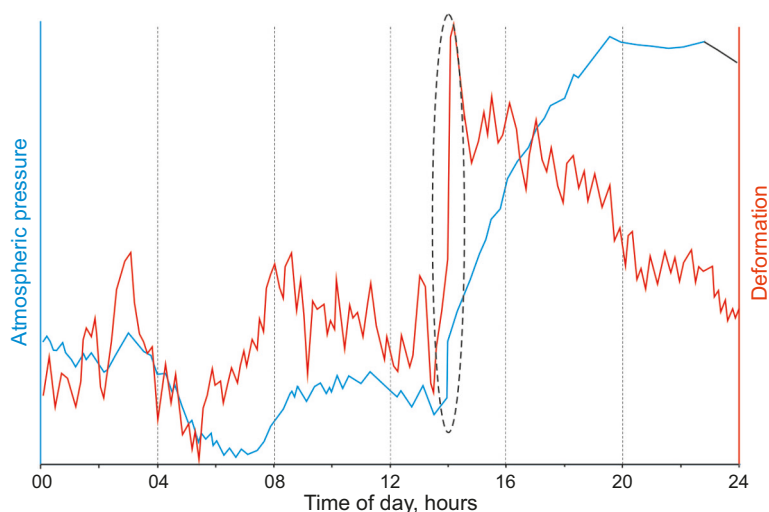


Fig. 8. Variations in atmospheric pressure (blue curve) and rock deformation (red curve). A black dashed ellipse marks a sharp increase in pressure and corresponding sharp increase of rock deformation.

Рис. 8. Вариации атмосферного давления (голубая кривая) и деформаций горных пород (красная кривая). Штрихпунктирный эллипс маркирует резкое увеличение давления и соответствующее ему резкое увеличение деформаций горных пород.

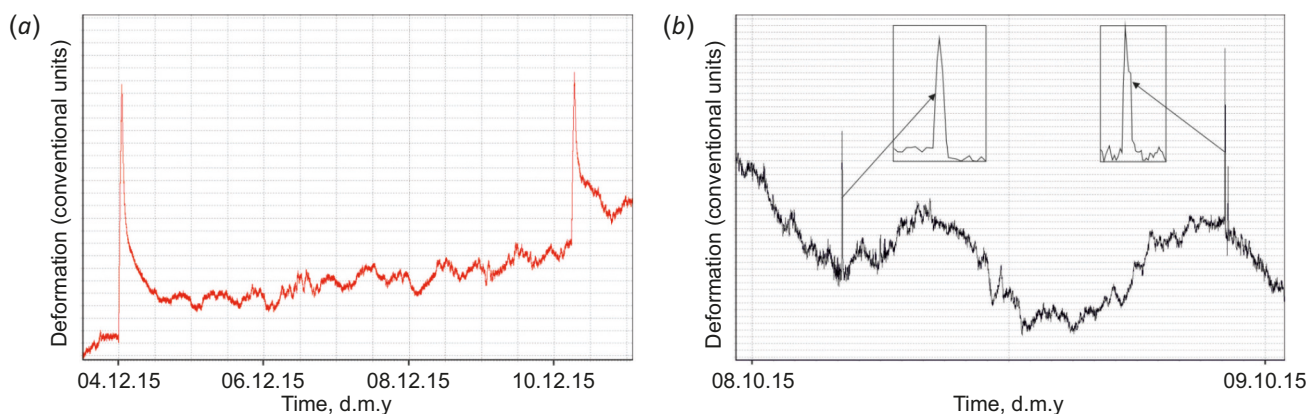


Fig. 9. Changes in rock deformation pulses caused by deformation waves of Type 1 (a) and Type 2 (b).

Рис. 9. Примеры импульсных изменений деформаций горных пород, обусловленных деформационными волнами первого (a) и второго (b) типа.

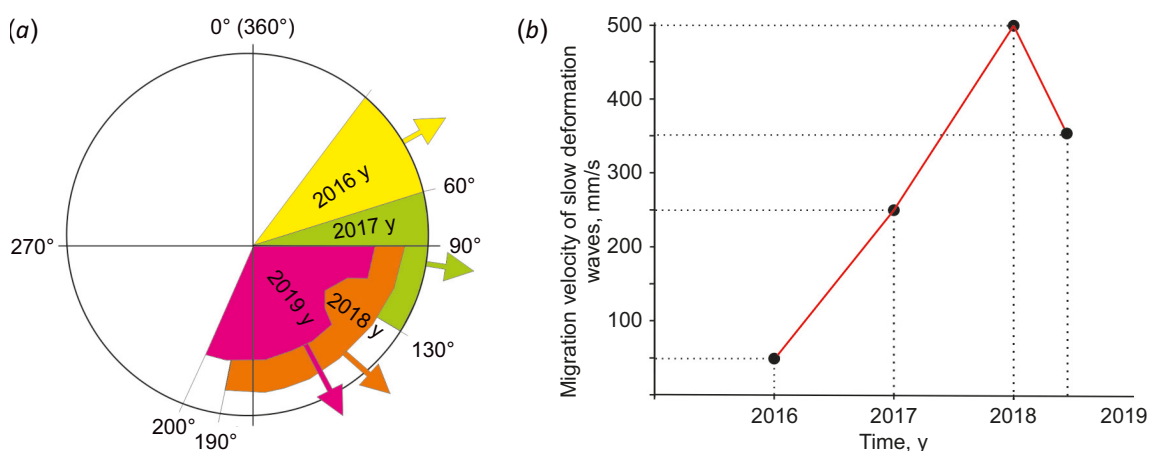


Fig. 10. Changes in the average vector (a) and average velocity of SDW spatial migration (b), based on the 2016–2019 dataset of the Talaya site.

Рис. 10. Изменение усредненных вектора пространственной миграции (a) и скорости (b) медленных деформационных волн в пункте «Талая» в 2016–2019 гг.

residual deformation with amplitude of a few microns. Type 1 waves are generated by sources located outside the monitored area. Probably, they are generated by tremor-like displacements along the faults located outside the monitored area [Peng, Gomberg, 2010]. Type 2 is detected as a symmetric or asymmetric pulse with amplitude of a few microns (Fig. 9, b). Such waves occur more frequently than those of Type 1 and are not accompanied by any residual deformation. They are presumably of a local nature related to stress redistribution in fault-block structures of the upper crust within the monitored area.

Periodic or permanent deformation occurs in the form of directionally propagating waves with an amplitude of the first microns and a length of 400–500 meters (according to approximate estimates) with velocities of a few centimeters to a few tens of centimeters per second. These velocities fall within the range of the maximum velocity estimates for permanently propagating slow deformation waves (SDWs) [Bykov, 2005]. The waves recorded at the monitoring sites in our study are SDWs, whose spatial migration directions and velocities vary in time. At the Talaya site, the SDW wave records show a 90° change in an average azimuth direction of the wave migration in the period of 2016 to 2019 (Fig. 10, a). Besides, the angle of the sector of possible azimuth solutions expanded from 20° in 2016 to 110° in 2019. A large scatter of the calculated SDW azimuth directions makes it impossible to define clearly the direction of the spatial migration in the first half of 2020. The most probable cause of this scatter is a high differentiation of the deformation fields in the study area due to a high level of stresses accumulated in the upper lithosphere before the Bystrinskoe earthquake. Our interpretation is indirectly confirmed by a change in the SDW spatial migration velocity that increased by an order of magnitude from 50 mm/s (2016) to 500 mm/s (2018) and decreased to 350 mm/s (2019) later on (Fig. 10, b).

6.2. Rock deformation signals before strong earthquakes

The Mw 6.3 Kultuk earthquake of August 27, 2008.

The rock deformation monitoring data of the Talaya site for the year of 2008 were used to investigate the Mw 6.3 Kultuk earthquake that occurred on August 27, 2008 at the southwestern termination of the Baikal Lake. The distance from the Talaya site to the epicenter is about 25 km. Three 1.83 m long bar sensors (ends fixed into the adit walls) were oriented in three mutually perpendicular directions, i.e. in (1) longitudinal (60° strike), (2) normal (50° strike), and (3) vertical directions. Measurements were taken every 30 s.

Figure 11 shows the signals (hour sampling) recorded by sensor 1 and provides a clear illustration of the deformation features before the earthquake, specifically three rock deformation trends (black dashed lines). About 50 days before the earthquake, trend 1 is replaced by trend 2, which indicates an acceleration of the deformation accumulation. Trend 2 is maintained for 42–43 days and then, 6–7 days before the earthquake, changes to trend 3 (Fig. 11). The deformation growth is terminated in this time interval, and the transition to the self-oscillation mode is indicative of self-organization in the deformation process (Fig. 11, inset).

The self-organization is confirmed by the results of monitoring data processing by two independent methods. Fig. 12 shows the result obtained by the structural functions curvature analysis method (SFCAM) [Vstovsky, 2006]. The first experience of using SFCAM for processing of rock deformation monitoring data is described in detail in [Bornyakov, Vstovsky, 2010]. Here, the physical sense of a structural function (SF) should be mentioned – the SF growth for small lags implies the appearance of temporary interrelations in the signal, which suggests coherent behavior of elements comprising the system analyzed. On the contrary, the cessation of SF growth for large lags implies failure

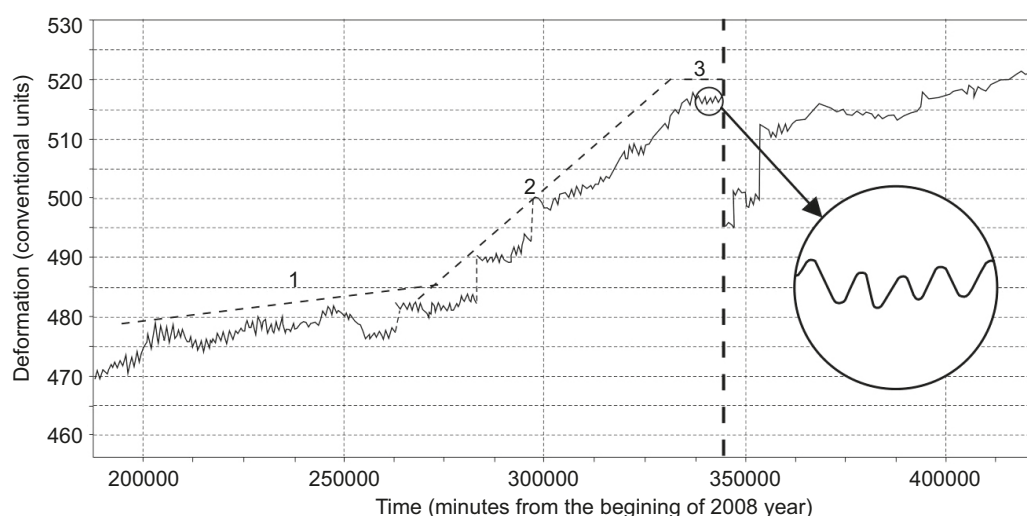


Fig. 11. Rock deformation vs time, according to the data of sensors 3 (Talaya site). The earthquake beginning (344732 minutes from the start of the year) is marked by a dashed line.

Рис. 11. Графики деформаций горных пород по показаниям датчиков 3 (пункт «Талая»). Пунктирной линией отмечен момент землетрясения (344732 мин).

of the interrelations. The conventional boundary of scale zones (determined by one or another rule or algorithm) is termed as correlation time (CT).

In Fig. 12, sharp CT changes are observed approximately 65000–70000 minutes (45–50 days) before the Kultuk earthquake. These changes vary in a wide range, from 1000 to 10000 minutes (Fig. 12). Two peak CT values in the time interval of 273000–285000 minutes (i.e. within 8 days) indicate two episodes of the appearance and failure of temporary interrelations in the deformation process, which most probably resulted from a significant re-arrangement of stress fields in the fault-block structure of the lithosphere, specifically in the focal area (which resulted in the earthquake). In this case, we can say that an intermediate-term (45–50 days) precursor of the Kultuk earthquake has been reliably detected from the rock deformation monitoring data.

Approximately one month (40000–45000 minutes) before the earthquake, the focal area reaches a metastable state, $CT=100$ –200 minutes. A sharp CT increase is observed ten days (14700 minutes) before the earthquake. The CT value still increases and reaches 6200 minutes six days (336000 minutes) before the earthquake (Fig. 12). This time point can be interpreted as the beginning of the early meta-instability substage, when the previously close interrelation in the deformation process begins to fail. This failure comes up to the time point of 340500 minutes. The beginning of a short-term recovery of the interrelation (three days before the earthquake) is the beginning of the late meta-instability substage.

Thus, the above SFCAM results show that CT variations reflect the features of the deformation process that develops in the fault-block medium, in which there is the development of an upcoming earthquake source. In particular, an anomalous growth of CT values is an indicator of the development of temporary interrelations of the deformation

time series data, which results from the self-organization of the deformation process. In case of the Kultuk earthquake, the self-organization took place twice – one month and a few days before the seismic event. These two episodes of self-organization were, respectively, intermediate- and short-term earthquake precursors.

Another method used for efficient computations from large and unevenly sampled datasets is the spectral analysis based on the Lomb–Scargle periodogram [Lomb, 1976; Scargle, 1982, 1989; Savransky, 2004; Press et al., 2007]. This method was successfully applied in our previous studies to process the rock deformation signals of sensor 3 before and after the Kultuk earthquake and indirectly confirmed the self-organization of the deformation process [Bornyakov et al., 2017]. For a more detailed spectral analysis, the rock deformation monitoring data collected from June 10 to October 9, 2008 were grouped into five datasets: June 10 – July 9 (a), July 10 – August 9 (b), August 10 – August 26 (pre-seismogenic time) (c), August 28 – September 9 (d), and September 10 – October 9, 2008 (e) (Fig. 13). It should be noted that the signals recorded on August 27, 2008 (earthquake date) did not participate in the analysis. Spectrograms show clearly that both structure and intensity of the oscillations change with time, especially in the range from E5 to 8E5 (Fig. 13), as follows:

June 10 – July 9 (Fig. 13, a): Six main periods of oscillations; the oscillation pattern is chaotic.

July 10 – August 9 (Fig. 13, b): Nine main periods; periodogram parameter 24hP begins to decrease; the oscillation pattern has an element of order.

August 10 – August 26 (Fig. 13, c): Pre-seismogenic state; parameter 24hP continues to decrease; the oscillation pattern is of a high degree of order, as shown by its fractal structure (see the inset). This implies that these rock deformation time series data are in a close temporary interrelation, and the oscillations are time-coordinated and

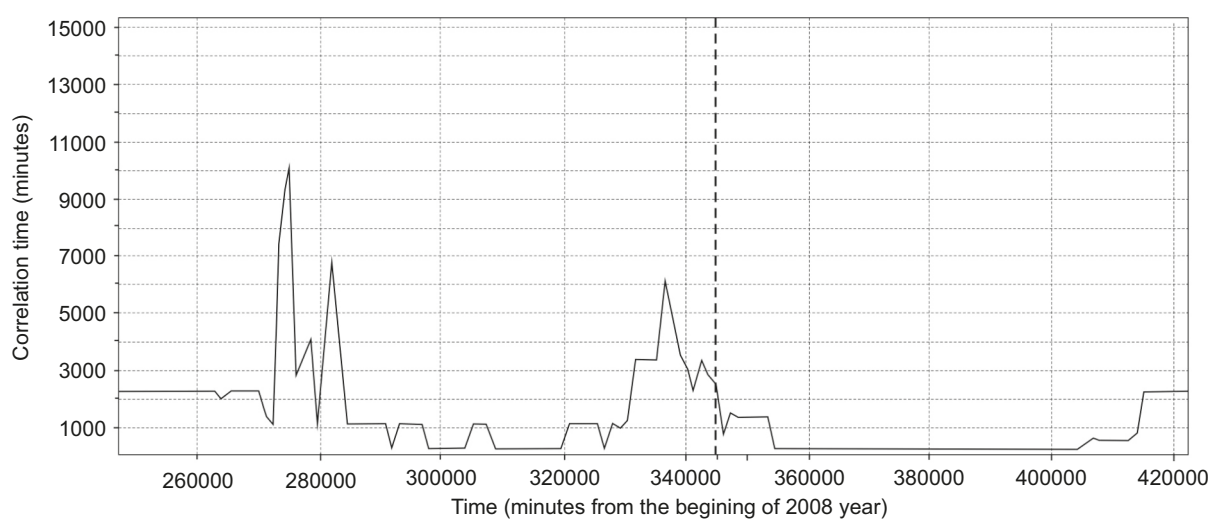


Fig. 12. Correlation time (CT) variations, according to the data of sensor 3 (Talaya site). The earthquake beginning (344732 minutes from the start of the year) is marked by the dashed line.

Рис. 12. График вариаций времени корреляции по данным датчика 3 (пункт «Талая»). Пунктирной линией отмечен момент землетрясения (344732 мин).

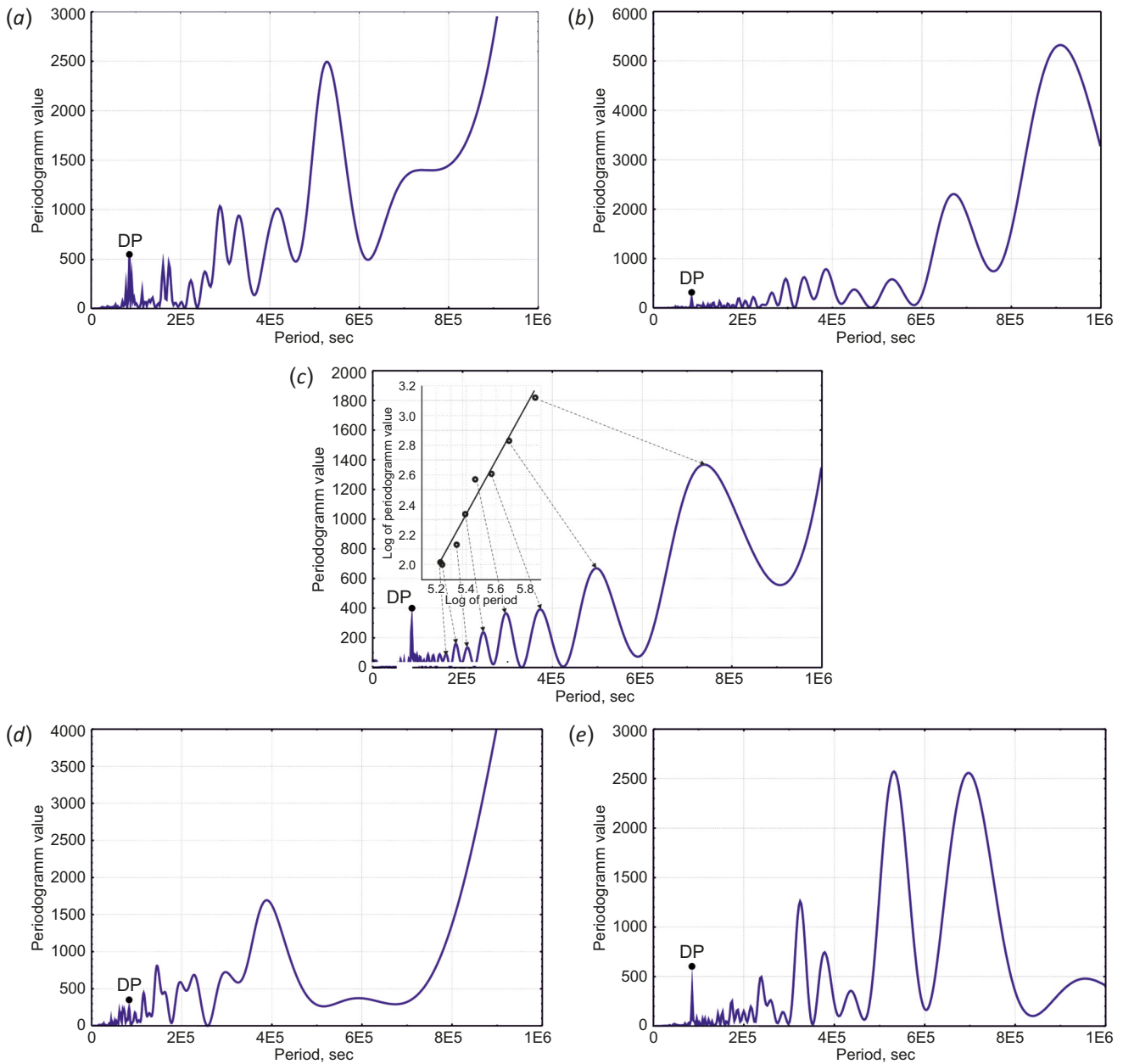


Fig. 13. Spectral analysis results for the rock deformation datasets. (a) – June 10 – July 9; (b) – July 10 – August 9; (c) – August 10 – August 26; (d) – August 28 – September 9; (e) – September 10 – October 9, 2008. DP – periodogram parameter (24-hours period).

Рис. 13. Результаты спектрального анализа данных деформаций горных пород для временных интервалов. (a) – 10 июня – 9 июля; (b) – 10 июля – 9 августа; (c) – 10 августа – 26 августа; (d) – 28 августа – 9 сентября; (e) – 10 сентября – 9 октября 2008 г. DP – суточный период.

intensity-adjusted. Here, we reveal the self-organization as a consequence of the deformation process before the earthquake, which is confirmed by the above-described SFCAM results (see Fig. 12).

August 28 – September 9 (Fig. 13, d): After the earthquake, there are significant changes in the rock deformation mode – the deformation process is very chaotic; the value of parameter 24hP is increased; short- and medium-period (0–4E5 sec) oscillations are dominant, and any long-period (4E5 до 1E5 sec) oscillations are lacking (or not manifested clearly).

September 10 – October 9 (Fig. 13, e): the deformation process tends to return to the original mode – this spectrogram is qualitatively similar to that for June 10 – July 9 (Fig. 13, a).

The analysis of the spectrograms with the focus on parameter 24hP reveals a specific pattern of its changes. In the spectrogram for June 10 – July 9, it is at the level of 600 minutes (Fig. 13, a). During two time intervals before the earthquake, it decreases to 350–400 minutes (Fig. 13, b, c). It remains at the same level for two weeks after the earthquake (Fig. 13, d), and increases again later on (Fig. 13, e).

The Mw 5.4 Bystrinskoe earthquake of September 21, 2020. The epicenter was located 18 kilometers from the Talaya site. Now we can say that the symptoms of this imminent seismic event were recorded six days before its occurrence, when eight out of ten sensors registered changes in the rate of deformation accumulation. The most distinct signals of anomalous changes in the deformation process were recorded by the sensors oriented to the focal area (sensors 1, 4, and 8), as illustrated here by the data of sensor 8 (Fig. 14).

From September 05 to September 16, 2020, the rock deformation developed against the background of 12-hour oscillations due to lunar-solar tides, and decreased by 5.0 microns. From September 16, the deformation began to grow. Some days before the earthquake, the deformation process accelerated, as evidenced by the daily increment of extension (Fig. 14). After the earthquake, the deformation began to decrease rapidly and gradually went down to the background values later on (Fig. 14).

The mechanism of the Bystrinskoe earthquake is determined as strike-slip [Bornyakov et al., 2021; Seminsky et al., 2021]. The processes of its generation and occurrence

are fully consistent with the synergistic interpretation of the stick-slip model [Ma et al., 2012, 2014]. The dynamics of the deformation process during six days before the seismic event, as recorded by the Talaya site, falls entirely within the early and late meta-instability substages of the final stage of meta-instability, according to the above-described concept of the earthquake source evolution. At the early meta-instability substage (September 16–20, 2020), the deformation process developed with a slow acceleration. At the late meta-instability substage (September 20), the deformation acceleration was significant. A short-term deceleration (for a few hours) took place immediately before the main shock of September 21 (Fig. 14, inset a).

It should be noted that the transition from the deformation process to the late meta-instability substage was preceded by a tremor-like displacement, as evidenced by a prolonged oscillation of the rock deformation signals (Fig. 14, inset b). A change in the information entropy is revealed in the deformation time series signals recorded on September 05–27, 2020 (Fig. 14, inset c). Its value remains high on September 05–13, which indicates that the deformation process is stationary during this period of time, thus

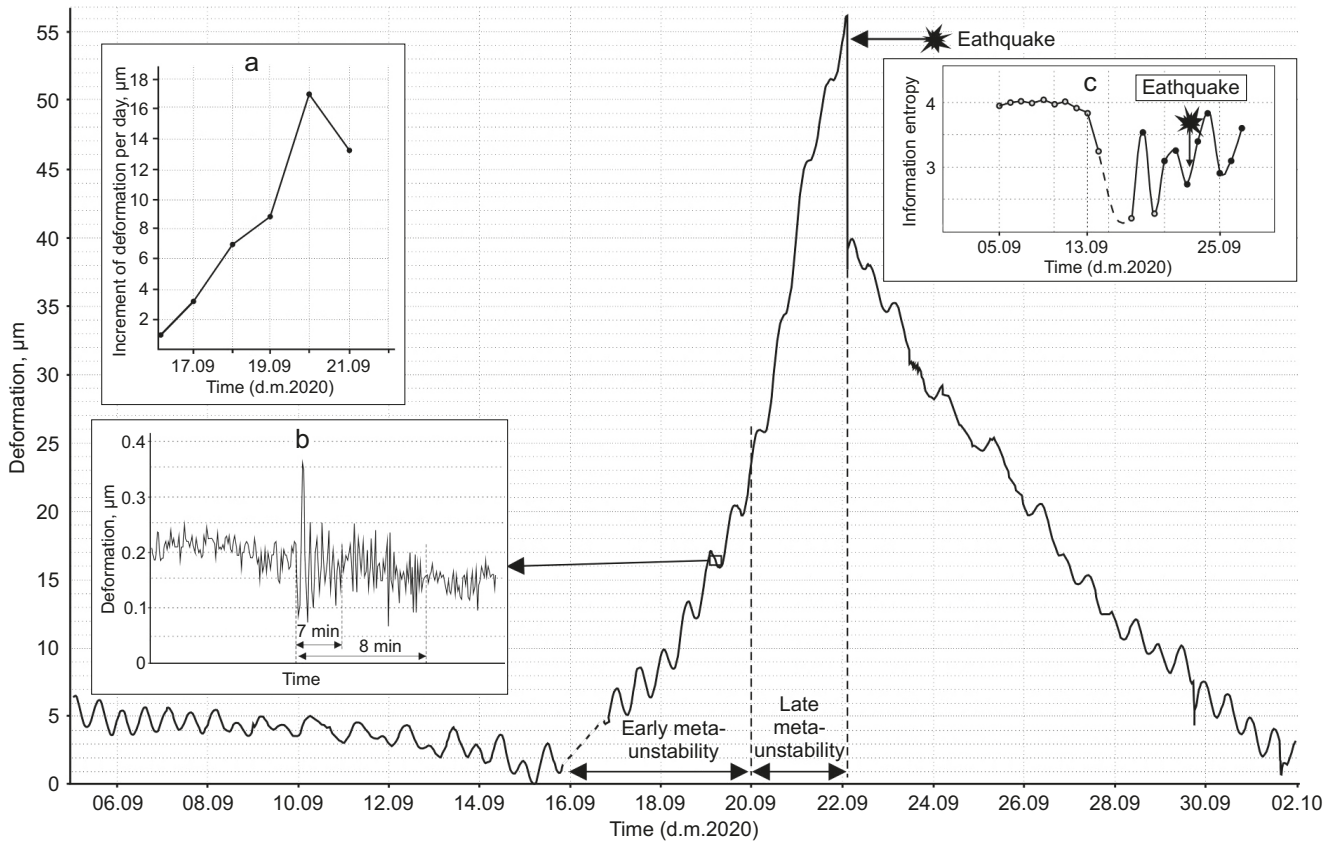


Fig. 14. Rock deformation signals recorded by sensor 8 (Talaya site) from September 5 to October 2, 2020. Insets: a – daily increase in rock deformation from September 16 to 22, 2020; b – deformation response of the rock mass in the adit to tremors in the source of the Bystrinskoe earthquake; c – change in the information entropy from September 5 to 27, 2020.

Рис. 14. График деформаций, зарегистрированных штанговым датчиком 8 с 5 сентября по 2 октября 2020 г. в штольне сейсмостанции «Талая». Врезки: а – график посуточного прироста деформаций с 16 по 22 сентября 2020 г.; б – деформационный отклик породного массива в штольне на тремор подобного смещения в очаге Быстринского землетрясения; с – изменение информационной энтропии с 5 по 27 сентября 2020 г.

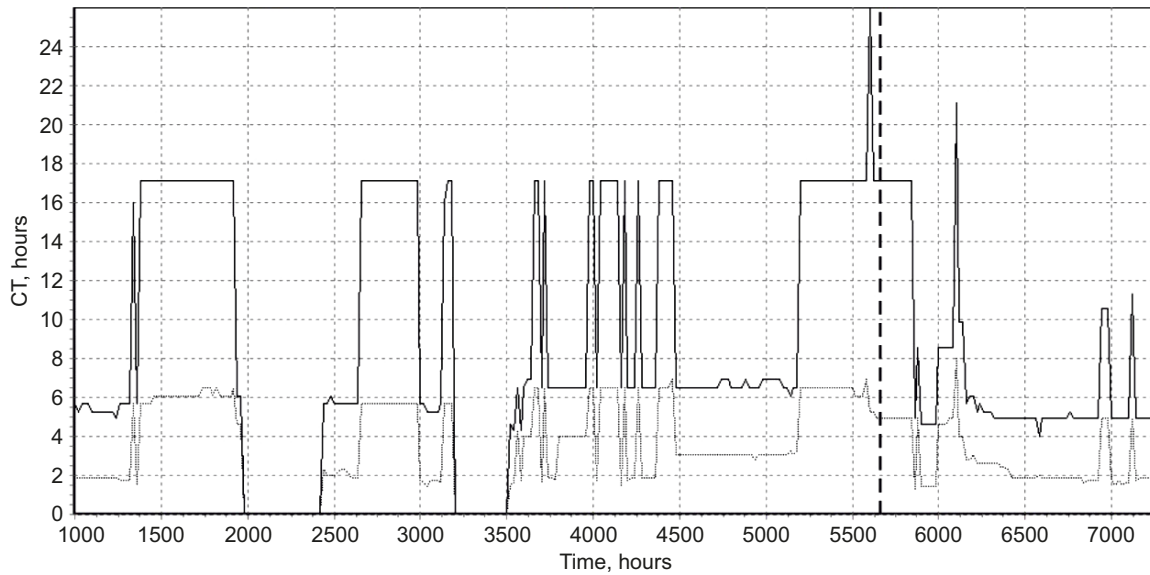


Fig. 15. Graph variation of correlation time. A vertical dashed line shows the moment of the Bystrinskoe earthquake. Time in hours, beginning from February 1.

Рис. 15. График вариаций времени корреляции. Вертикальной пунктирной линией отмечен момент Быстринского землетрясения. Время дано в часах от 1 февраля.

corresponding to the metastable stage. From September 13 to 14, the information entropy values sharply drop down, which implies the beginning of transition to the metastable stage. This is 2–3 days ahead of the beginning of the transition (September 16–17), which can be visually detected from the change in the deformation trend from decreasing to increasing (Fig. 14). Apparently, information entropy is sensitive to insignificant changes in the deformation process, although these may not always be explicitly manifested. The next two significant variations of this parameter correlate with two episodes of significant restructuring of the deformation process before the earthquake.

In this case, the rock deformation monitoring data clearly show the final meta-instability stage of the Bystrinskoe earthquake generation, which is reflected in the regular dynamics pattern of the deformation process. Our study shows that anomalous deformation signals follow a specific spatiotemporal pattern and allow identifying the early and late meta-instability substages. Here, the anomalous deformation signals and accompanying tremors are actually the short-term precursors of an imminent strong earthquake.

Deformation monitoring data in the time interval from 01.02. 2020 to 30.10.2020, 2020, including the Bystrinsky earthquake, were processed by the MAKSF method and the spectral analysis method.

The obtained graph of the correlation time differs from the previous one in terms of the values of the CT parameter and the frequency of its variations (see Fig. 10; Fig. 15). Thus, in the final phase of the preparation of the Bystrinsky earthquake, the process of deformation self-organization took place within 18 days (CT = 450 hours), whereas in the case of the Kudarin earthquake, such self-organization had a more transient character, most intensively manifested three days before it. These differences are probably due

to the different mechanisms and magnitudes of the Kultuk and Bystrinsky earthquakes. Without going into details, we note that the Bystrinsky earthquake was preceded by several time intervals where the processes of self-organization manifested themselves. The last of these began at 5150 o'clock (at the end of August) with a sharp increase three days before the earthquake (mark 5558 hours on the chart) (Fig. 15).

For the spectral analysis, the time series was divided into the following intervals: June 1–30 – July 1–31, July 1–10 – August 1–31, and September 1–20 – September 22–30 – October 1–30. The spectral analysis was made on each data sample (Fig. 16). The spectrograms presented show temporal changes in the structure and intensity of oscillations which are most clearly defined for the periods in the interval E5 to E6. The first spectrogram in this interval shows four fundamental periods with the periodogram parameter value larger than 1000 (Fig. 16, a). In the next time interval, the periods number increases to five, due to the emergence of additional period 1.6E6, with the periodogram parameter value increased twice against the background of increasing spectrogram randomization. In the third interval, the number of fundamental periods of oscillations with the periodogram parameter value greater than 1000 increases to eight, and the spectrogram structure attains regularity (see Fig. 14, b) similar to that shown in Fig. 11, b. In the next pre-siesmogenic interval, this regularity remains unchanged against the background of the periodogram parameter value increased to more than twice (Fig. 16, d). After the earthquake, there occurs a reconstruction of the spectrum structure. In the last decade of September, only long-period oscillation 4E5 remains important (Fig. 16, e). In the subsequent calculation period, there is a considerable decrease of the periodogram

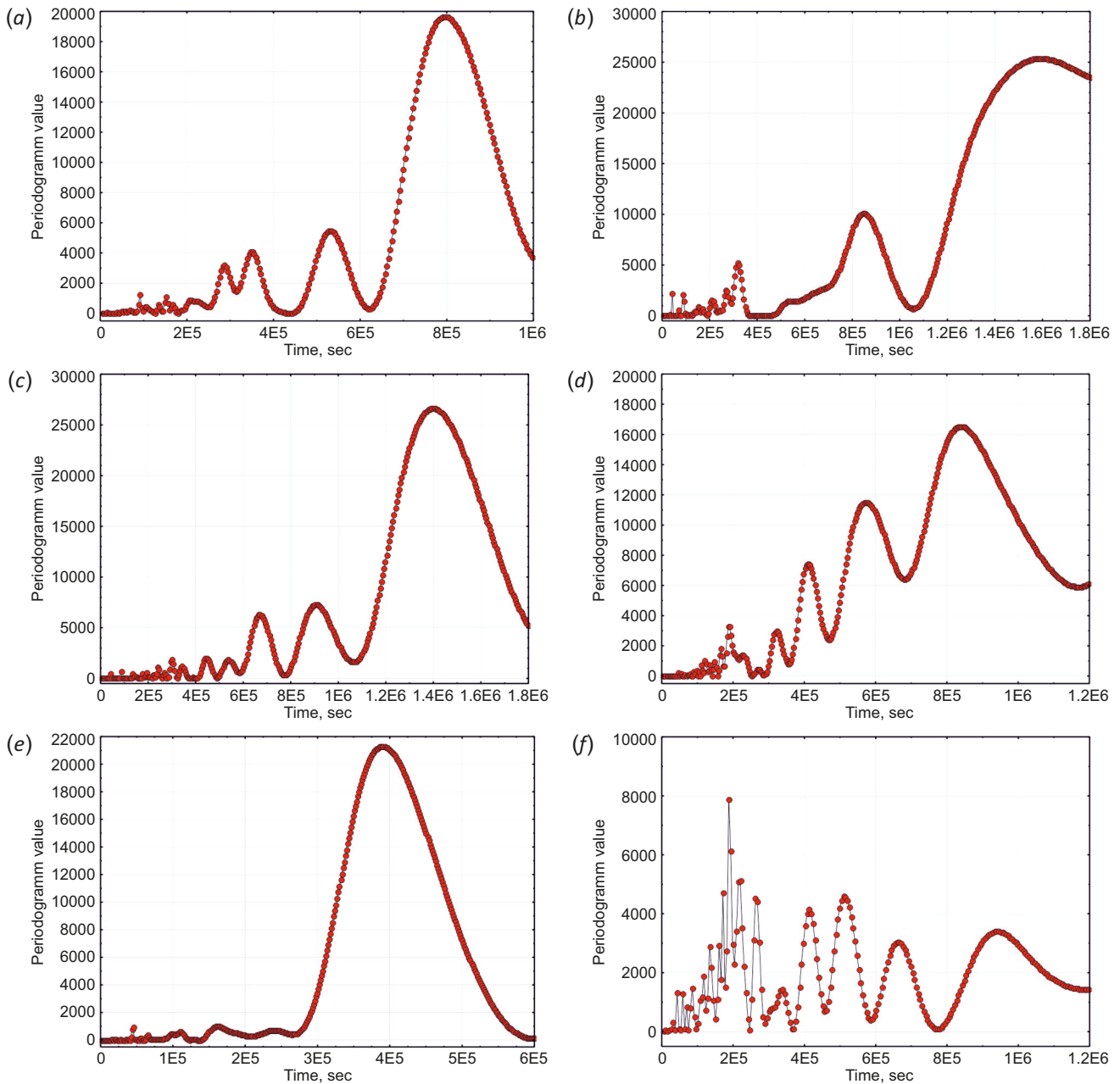


Fig. 16. Spectral analysis results for the rock deformation datasets for the Talaya site: (a) – June 1–30, (b) – July 1–30, (c) – August 1–31, (d) – September 1–20, (e) – September 22–30, (f) – October 1–30, 2020.

Рис. 16. Результаты спектрального анализа данных деформаций горных пород в пункте «Талая» для временных интервалов: (a) – 1–30 июня, (b) – 1–31 июля, (c) – 1–31 августа, (d) – 1–20 сентября, (e) – 22–30 сентября, (f) – 1–30 октября, 2020.

parameter value, and the spectrogram acquires an irregular structure with the short-period oscillation predominance (Fig. 16, f).

The Mw 5.5 Kudara earthquake of December 10, 2020. Several seismological agencies have investigated the Kudara earthquake by modeling the volume and surface deformation waves. Their focal mechanism solutions are consistent with each other and mostly show the NW-SE crustal extension and normal faulting in the source, with an insignificant strike-slip component.

The earthquake generation is reflected in the rock deformation monitoring records of the Buguldeika and Olkhon

sites, both located 40 km away from the epicenter (see Fig. 3, a) Although the distance between these sites is small (26 km), there is a difference in their records before the occurrence of the seismic event. The data of the Buguldeika site show sinusoid-shaped oscillations with an increase in the oscillation amplitude during 30 days before the earthquake (Fig. 17, a, b). In the records of sensor 1 at the Olkhon site, an exponential increase in deformation is detectable ten days before the earthquake (Fig. 17, c), which is similar to the deformation increase recorded by the Talaya site before the Bystrinskoe earthquake (see Fig. 14) (note that there are some differences in their deformation dynamics in time).

The records of sensor 2 of the Olkhon site do not show any visual signs suggesting an upcoming earthquake.

These differences in the deformation signals of the earthquake generation are due to the fact that the Buguldeika and Olkhon sites are located in different structural settings. The Buguldeika site is placed at the intersection of two local fault zones in the wedge-shaped crustal block bordered

by the Primorsky and Morsky regional faults (see Fig. 3, d). As mentioned above (see Section 4. Structural-geodynamic settings), the shear amplitude of the Morskoy fault is large, and the SE upper part of the block is in contact with the lake water body and the sediments of the South Baikal depression, which hinder the propagation of the SE-trending regional extension from the Transbaikalia area to this block.

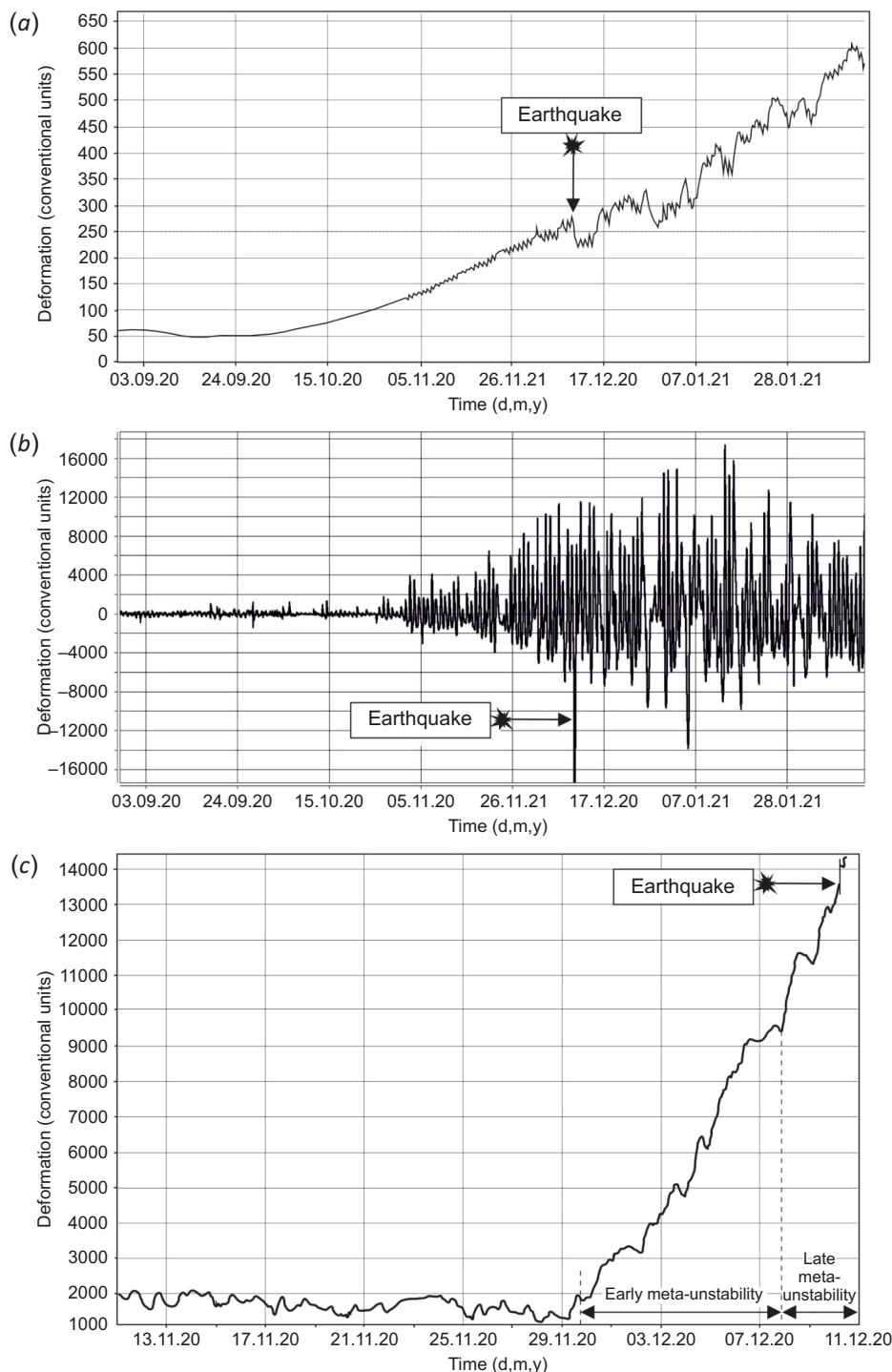


Fig. 17. Rock deformation vs time. Data of sensor 1 (Buguldeika site) before and after data filtering ((a) and (b), respectively) (except for more than one hour fluctuations). (c) – data of sensor 1 (Olkhon site).

Рис. 17. Изменение деформаций горных пород во времени согласно тензодатчику 1 в пункте мониторинга «Бугульдейка» до (a) и после фильтрации данных с исключением колебаний с периодом более 1 часа (b), а также в точке 1 пункта «Приольхонье» (c).

The oscillatory nature of the rock deformation signals recorded before the Kudara earthquake is of a secondary nature and due to "swinging" of the block in response to the increased extension of its lower horizons (Fig. 17, a, b). The oscillations began two months before the earthquake and continued for three months after its occurrence.

The Olkhon site is located in the local fault zone that belongs to the regional Primorsky fault zone. As the distance to the Morsky fault scarp is 14–15 km, this location is subjected to the regional extension. In the records of sensor 1, the generation of the Kudara earthquake is reflected as a sharp increase in rock deformation. At this location,

directly in the fault, the deformation dynamics before the earthquake corresponds to the early and late meta-instability substages in the stick-slip model [Ma et al., 2014]. In the undisturbed block, sensor 2 recorded no anomalous changes in deformation. The lack of an obvious response to the earthquake generation is due to the fact that crustal blocks, in contrast to faults, are less prone to immediate response to changes in the local stress field.

The spectral characteristics of the deformation time series before and after the Kudara earthquake involved the September 2020 to January 2021 deformation monitoring results obtained from the Buguldeika site. The entire time

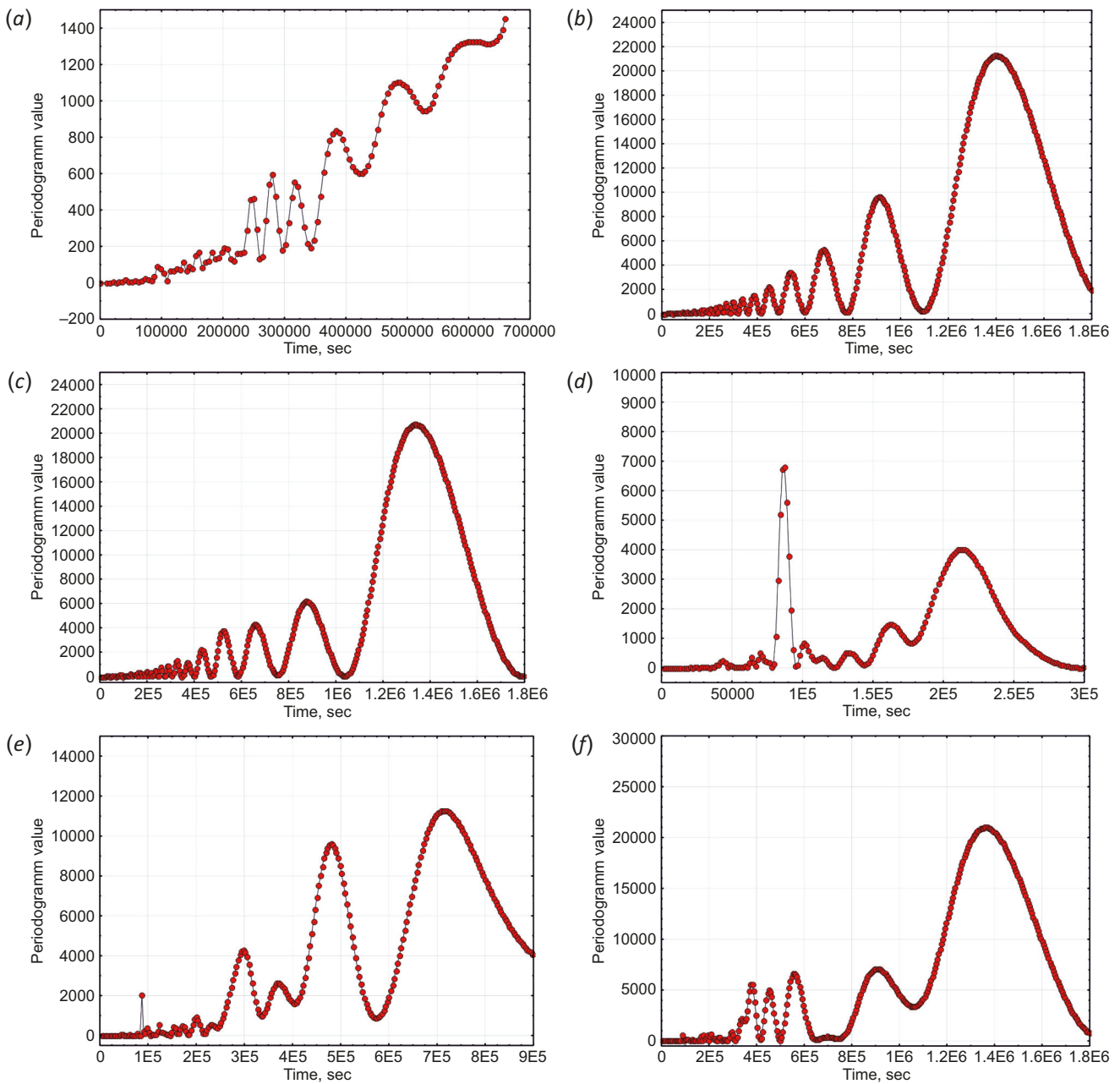


Fig. 18. Spectral analysis results for the rock deformation datasets for Buguldeika site: (a) – September 1–30, (b) – October 1–31, (c) – November 1–30, (d) – December 1–9, (e) – December 11–31, (f) – January, 1–31, 2020.

Рис. 18. Результаты спектрального анализа данных деформаций горных пород в пункте Бугульдейка для временных интервалов: (a) – 1–30 сентября, (b) – 1–31 октября, (c) – 1–30 ноября, (d) – 1–9 декабря, (e) – 11–31 декабря, (f) – 1–31 января, 2020.

series was divided into the following intervals: September 1–30 – October 1–31, November 1–30, December 1–9, December 11–31, and January 1–31. The spectral analysis was made on each data sample (Fig. 18). The spectrograms presented show temporal changes in the structure and intensity of oscillations. As in the previous cases, this is most evident for the periods in the interval E5 to E6. In the interval 2E5 to 7E5 of the first spectrogram, there are only two fundamental periods with the periodogram parameter value greater than 1000 (Fig. 18, a). The fundamental periods number increases to nine due to the emergence of seven additional fundamental periods of oscillations in the interval 3E5 to 1.6E6, with the periodogram parameter value increased more than twice and the spectrogram itself acquired a regular structure (Fig. 18, b). In the third interval, the spectrogram structure generally remains unchanged, with a small decrease in the periodogram parameter value for some of the periods (Fig. 18, c). The structural ordering characteristic of the pre-seismogenic state is absent on the next spectrogram obtained during the ten-day time interval preceding the earthquake.

There are no period values greater than 2.2E5 on the seismogram, and lesser period values increased 3–4 times as compared to the previous spectrograms (Fig. 18, b, c, d). It is worthy of note that daily oscillations in that time interval are of considerable importance (Fig. 18, d). After the earthquake, there occurs a reconstruction of the spectrum structure. In two last decades of December and in January, there is a gradual increase in the number of long-period oscillations and an increase of the periodogram parameter value (Fig. 18, e, f), with the spectrogram structure remained random.

The direct instrumental observations of the rock deformations and the spectral analysis results generally show that the time series of the deformation monitoring have multicomponent structure (see Figs. 7, 9, 10, 13, 16, 18). Rock deformations occur in the form of the oscillation process with a wide spectrum of single-mode random and regular oscillations which have a wide range of periods. Among those are multi-day, daily and shorter, up to second-order, oscillations. This process has a time-varying structure. The variation involves the sets of periods considered and their importance in the deformation process as a whole. An important functional feature of this process is that the structure of oscillation spectrum becomes regular before large earthquakes.

7. DISCUSSION

Attempts to develop a technology for short-term earthquake prediction have so far been unsuccessful, despite much effort towards searching for precursors. The global experience of research and seismic observation shows that the currently known precursors occur selectively and inconsistently. Creating an effective technology is challenging yet possible, pending a discovery of a universal precursor that always and inevitably occurs and is detectable in various structural and geodynamic settings, if not any, then at least of the same type.

In the theoretical approach applied here to search for possibilities to develop a technology for short-term earthquake prediction (see Section 1), self-organization is an integral property of the deformation process. It is reflected in the critical pre-seismogenic state of the fault-block structure in an area wherein the source of an impending earthquake is developing. The self-organization in the deformation process takes place several days before a seismic event and is detectable by direct and indirect methods [Bornyakov, Vstovsky, 2010; Bornyakov et al., 2017].

Compared to the self-organization, all other known precursors (that are not its derivatives) have a lower capability of providing predictive information because their manifestation is highly variable in both space and time, and should be thus taken into account only as secondary and/or occasional. Such precursors detectable by deformation monitoring are the above-described separate wave impulses generated by tremors in the earthquake source, as well as specific changes in the parameters of permanently propagating slow deformation waves (SDWs).

The experimental data show that tremors take place at the meta-instability stage, i.e. when a displacement along the rupture is being generated [Ma et al., 2014; Zhuo et al., 2019]. Depending on the duration of this stage in nature, the tremors can be considered as intermediate and/or short-term precursors. These findings based on the laboratory modeling data are consistent with the well-known instrumental observations [Bornyakov et al., 2019; Gombert et al., 2008; Idehara et al., 2014; Sun et al., 2015].

Permanently propagating SDWs are indicators of the stress-strain state of the fault-block medium. The azimuth direction of SDW migration reflects the predominant direction of the active vector of deformation, and an increase in the migration velocity in time indicates an increase in the stress level. In 2019, the state of the lithosphere in the study area was assessed as pre-seismogenic [Bornyakov et al., 2019]. This conclusion was based on the analysis of the change in the azimuth direction of the averaged deformation vector in the study area in 2016–2019 (see Fig. 10, a) and a ten-fold increase in the SDW migration velocity (see Fig. 10, b). It was confirmed by the occurrence of the Bystrinskoe and Kudara earthquakes in 2020. This is a reason to consider the above-specified temporal changes of the two parameters of permanently propagating SDWs – deformation direction and migration velocity – as long-term precursors of earthquakes.

Occasional precursors, unlike the inevitable one, are influenced by various factors, including the structural-geodynamic setting of a monitoring site and its position relative to an earthquake source.

The influence of the structural-geodynamic setting is clearly seen in the deformation records of the Buguldeika and Olkhon sites before the Kudara earthquake. Despite the same distance from its epicenter, the rock deformation at these two sites was different due to their different structural conditions (see Figs. 3, 14, 15). At the same time, within the area monitored by the Olkhon site, the earthquake was preceded by an intense rock deformation only on the site

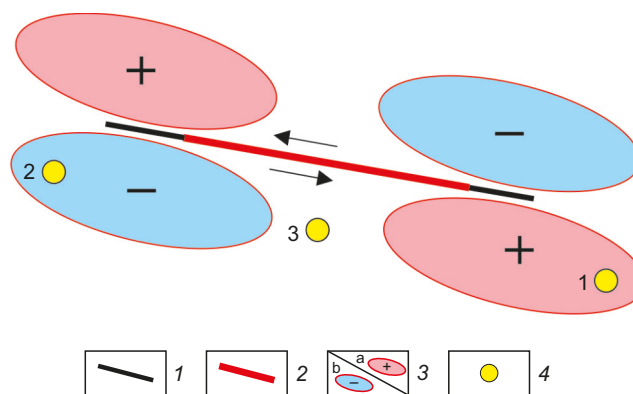


Fig. 19. Three locations of deformation monitoring sites relative to a seismogenically activated fault segment.

1 – fault; 2 – seismogenically activated segment; 3 – areas of horizontal compression (a) and tension (b); 4 – rock deformation monitoring site.

Рис. 19. Три варианта расположения пункта деформационного мониторинга относительно сейсмогенно активизированного сегмента разлома.

1 – разлом; 2 – сейсмогенно-активизированный сегмент разлома; 3 – области горизонтального сжатия (a) и растяжения (b); 4 – пункт деформационного мониторинга.

located in the fault zone, while no deformation occurred on the site located in the block bordering the fault zone (see Fig. 15).

Fig. 19 shows three positions of monitoring sites relative to a seismogenically activated fault segment with a left-lateral shear (i.e. relative to potential earthquake epicenters). Before an earthquake, monitoring site 1 can record an intensive increase in compression deformation in the direction of the future seismogenic displacement. It should be noted that this position is fully similar to that of the Talaya site relative to the epicenter of the Bystrinskoe earthquake (see Figs. 3, 14). On the contrary, monitoring site 2 can record rock extension. At site 3, deformation is weak and chaotic, without clearly expressed precursors.

8. CONCLUSION

In our approach to creating a technology for short-term forecasting of earthquakes, we suggest that the main and inevitable precursor of an earthquake is the self-organization in the deformation process, i.e. the occurrence of self-organized initial micro-foci of destruction in the fault plane immediately before its seismogenic activation. The coherent behavior of the micro-foci of destruction is detectable from rock deformation monitoring data by special analysis methods adapted to identifying time intervals with correlations of an analyzed parameter in the time series of the deformation data. In the case of strong tectonic earthquakes, this precursor is inevitable and always present before an earthquake, regardless of earthquake mechanism types. All other precursors considered as secondary or occasional are influenced by various factors and do not always occur before a seismic event. As confirmed by the above-described deformation monitoring data analysis, such factors are the structural-geodynamic settings of monitoring sites and their positions relative to an earthquake source. Despite their random and selective occurrence, the occasional precursors are important for earthquake prediction

studies and should be considered in connection with the inevitable precursor.

In general, the study results presented here show that the proposed synergistic interpretation of the stick-slip model [Ma et al., 2012, 2014] gives the most adequate description of the process of periodic seismogenic activation of faults and can be used as the basis for a technology of short-term earthquake prediction.

9. CONTRIBUTION OF THE AUTHORS / ЗАЯВЛЕННЫЙ ВКЛАД АВТОРОВ

The authors contributed equally to this article.

Все авторы внесли эквивалентный вклад в подготовку публикации.

10. CONFLICT OF INTERESTS / КОНФЛИКТ ИНТЕРЕСОВ

The authors have no conflicts of interest to declare. All authors have read and agreed to the published version of the manuscript.

Авторы заявляют об отсутствии у них конфликта интересов. Все авторы прочитали рукопись и согласны с опубликованной версией.

11. REFERENCES

Bak P, Tang C., 1989. Earthquakes as a Self-Organized Critical Phenomenon. *Journal of Geophysical Research: Solid Earth* 94 (B11), 15635–15637. <https://doi.org/10.1029/JB094iB11p15635>.

Bornyakov S.A., 2008. Dynamic Criteria for the Self-Organization of Crack Systems in the Shear Zone (According to the Results of Physical Modeling). *Doklady Earth Sciences* 420, (6), 822–824 (in Russian) [Борняков С.А. Динамические критерии самоорганизации систем разрывов в сдвиговой зоне (по результатам физического моделирования) // Доклады АН. 2008. Т. 420. № 6. С. 822–824].

Bornyakov S.A., Dobrynina A.A., Seminsky K.Zh., San'kov V.A., Radziminovich N.A., Salko D.V., Shagun A.N., 2021. The Bystrinskii Earthquake in the Southern Baikal Region (Sep. 21, 2020, $M_w=5.4$): General Characteristics, Basic Parameters, and Deformation Signs of the Transition of the Focus to the Meta-Unstable State. *Doklady Earth Sciences* 498, 427–431. <https://doi.org/10.1134/S1028334X21050044>.

Bornyakov S.A., Ma J., Miroshnichenko A.I., Guo Y., Salko D.V., Zuev F.L., 2017. Diagnostics of Meta-Instable State of Seismically Active Fault. *Geodynamics & Tectonophysics* 8 (4), 989–998 (in Russian) [Борняков С.А., Ма Ц., Мирошниченко А.И., Гуо Ю., Салко Д.В., Зуев Ф.Л. Диагностика метанестабильного состояния сейсмоактивного разлома. *Геодинамика и тектонофизика*. 2017. Т. 8. № 4. С. 989–998]. <https://doi.org/10.5800/GT-2017-8-4-0328>.

Bornyakov S.A., Miroshnichenko A.I., Salko D.V., 2016. Diagnostics of the Preseismogenic State of Heterogeneous Media According to Deformation Monitoring Data. *Doklady Earth Sciences* 468, 481–484. <https://doi.org/10.1134/S1028334X16050032>.

Bornyakov S.A., Salko D.V., Shagun A.N., Dobrynina A.A., Usynin L.A., 2019. Slow Deformation Waves as a Possible Precursor of Seismic Danger. *Geosystems of Transition Zones* 3 (3), 267–276 (in Russian) [Борняков С.А., Салко Д.В., Шагун А.Н., Добрынина А.А., Усынин Л.А. Медленные деформационные волны как возможный предвестник сейсмической опасности // *Геосистемы переходных зон*. 2019. Т. 3. № 3. С. 267–276]. <https://doi.org/10.30730/2541-8912.2019.3.3.267-276>.

Bornyakov S.A., Vstovskii G.V., 2010. The First Experiment of Seismodeformational Monitoring of the Baikal Rift Zone: Example of the August 27, 2008, South-Baikal Earthquake. *Doklady Earth Sciences* 431, 469–473. <https://doi.org/10.1134/S1028334X10040136>.

Brace W.F., Byerlee J.D., 1966. Stick-slip as a Mechanism for Earthquake. *Science* 153, 990–992.

Brillouin L., 1966. *Scientific Uncertainty and Information*. Mir, Moscow, 271 p. (in Russian) [Бриллюэн Л. Научная неопределенность и информация. М.: Мир, 1966. 271 с.].

Bukharov A.A., 1996. Cenozoic Development of Baikal According to Results of Deep-Water and Seismostratigraphic Studies. *Russian Geology and Geophysics* 37 (12), 98–107 (in Russian) [Бухаров А.А. Кайнозойское развитие Байкала по результатам глубоководных и сейсмостратиграфических исследований // *Геология и геофизика*. 1996. Т. 37. № 12. С. 98–107].

Vukov V.G., 2005. Strain Waves in the Earth: Theory, Field Data, and Models. *Russian Geology and Geophysics* 11, 1158–1170.

Cicerone R.D., Ebel J.E., Britton J., 2009. A Systematic Compilation of Earthquake Precursors. *Tectonophysics* 476 (3–4), 371–396. <https://doi.org/10.1016/j.tecto.2009.06.008>.

Ciliberto S., Laroche C., 1994. Experimental Evidence of Self-Organization in the Stick-Slip Dynamics of Two Rough Elastic Surface. *Journal De Physique I* 4, 223–235. <https://doi.org/10.1051/JP1%3A1994134>.

Feder H.J.S., Feder J., 1991. Self-Organized Criticality in Stick-Slip Process. *Physical Review Letters* 66 (20), 2669–2672. <https://doi.org/10.1103/PhysRevLett.66.2669>.

Fomin Yu.N., Semibalamut V.M., Zhmud V.A., Panov S.V., Parushkin M.D., Dimitrov L.V., 2019. The Results of Deformation Measurements in the Gallery at the Talay Observatory. *Automatics & Software Engineering* 1 (27), 65–75 (in Russian) [Фомин Ю.Н., Семибаламут В.М., Жмудь В.А., Панов С.В., Парушкин М.Д., Димитров Л.В. Результаты деформографических измерений в штольне на обсерватории Талая // *Автоматика и программная инженерия*. 2019. № 1 (27). С. 65–75].

Geller R.G., Jackson D.D., Ragan Y.Y., Mulargia F., 1997. Earthquake Cannot Be Predicted. *Science* 275 (5306), 1616. <https://doi.org/10.1126/science.275.5306.1616>.

Gomberg J., Rubinstein J.L., Peng Z.G., Creager K.C., Vidale J.E., Bodin P., 2008. Widespread Triggering of Non-volcanic Tremor in California. *Science* 319 (5860), 173. <https://doi.org/10.1126/science.1149164>.

Haken H., 1978. *Synergetics*. Springer, 355 p. <https://doi.org/10.1007/978-3-642-96469-5>.

Haken H., 1983. *Advanced Synergetics: Instability Hierarchies of Self-Organizing Systems and Devices*. 2nd Edition. Springer, 356 p. <https://doi.org/10.1007/978-3-642-45553-7>.

Idehara K., Yabe S., Ide S., 2014. Regional and Global Variations in the Temporal Clustering of Tectonic Tremor Activity. *Earth, Planets and Space* 66, 66. <https://doi.org/10.1186/1880-5981-66-66>.

Logachev N.A., 1999. Main Structural Features and Geodynamics of the Baikal Rift Zone. *Physical Mesomechanics* 2 (1–2), 163–170 (in Russian) [Логачев Н.А. Главные структурные черты и геодинамика Байкальской рифтовой зоны // *Физическая мезомеханика*. 1999. Т. 2. № 1–2. С. 163–170].

Lomb N.R., 1976. Least-Squares Frequency Analysis of Unequally Spaced Data. *Astrophysics and Space Science* 39, 447–462. <https://doi.org/10.1007/BF00648343>.

Ma J., Guo Y., Sherman S.I., 2014. Accelerated Synergism along a Fault: A Possible Indicator for an Impending Major Earthquake. *Geodynamics & Tectonophysics* 5 (2), 387–399 (in Russian) [Ма Ц., Гуо Я., Шерман С.И. Ускоренный синергизм вдоль разлома: возможный индикатор неизбежного крупного землетрясения. *Геодинамика и тектонофизика*. 2014. Т. 5. № 2. С. 387–399]. <https://doi.org/10.5800/GT-2014-5-2-0134>.

Ma J., Sherman S.I., Guo Y.S., 2012. Identification of Meta-Instable Stress State Based on Experimental Study of Evolution of the Temperature Field during Stick-Slip Instability on a Bending Fault. *Science China Earth Sciences* 55, 869–881. <https://doi.org/10.1007/s11430-012-4423-2>.

Mandelbrot B.B., 1982. *The Fractal Geometry Nature*. W.H. Freeman & Co, San Francisco, 480 p.

Myachkin V.N., 1978. *Earthquake Preparation Processes*. Nauka, Moscow, 231 p. (in Russian) [Мячкин В.Н. Процессы подготовки землетрясений. М.: Наука, 1978. 231 с.].

Olami Z., Feder H.J.S., Christensen K., 1992. Self-Organized Criticality in a Continuous, Nonconservative Cellular

Automaton Modeling Earthquakes. *Physical Review Letters* 68 (8), 1244. <https://doi.org/10.1103/PhysRevLett.68.1244>.

Peng Z., Gombert J., 2010. An Integrated Perspective of the Continuum between Earthquakes and Slow-Slip Phenomena. *Nature Geoscience* 3, 599–607. <https://doi.org/10.1038/ngeo940>.

Press W.H., Teukolsky S.A., Vetterling W.T., Flannery B.P., 2007. *Spectral Analysis of Unevenly Sampled Data*. In: *Numerical Recipes. The Art of Scientific Computing*. Cambridge University Press, New York, p. 685–692.

Prigogine I., Kondepudi D., 2002. *Modern Thermodynamics. From Heat Engines to Dissipative Structures*. Mir, Moscow, 460 p. (in Russian) [Пригожин И., Кондепуди Д. Современная термодинамика: от тепловых двигателей до диссипативных структур. М.: Мир, 2002. 460 с.].

Psakhie S.G., Ruzhich V.V., Shilko E.V., Astafurov S.V., Smekalin O.P., 2004. Study of the Influence of Water Saturation and Vibrations on the Displacement Regime in Fault Zones. *Physical Mesomechanics* 7 (1), 23–30 (in Russian) [Псахье С.Г., Ружич В.В., Шилько Е.В., Астафуров С.В., Смекалин О.П. Изучение влияния водонасыщения и вибраций на режим смещений в зонах разломов // Физическая мезомеханика. 2004. Т. 7. № 1. С. 23–30].

Psakhie S.G., Ruzhich V.V., Smekalin O.P., Shilko E.V., 2001. Response of the Geological Media to Dynamic Loading. *Physical Mesomechanics* 4 (1), 67–71 (in Russian) [Псахье С.Г., Ружич В.В., Смекалин О.П., Шилько Е.В. Режимы отклика геологических сред при динамических воздействиях // Физическая мезомеханика. 2001. Т. 4. № 1. С. 67–71].

Ruzhich V.V., 2004. High-Precision Measuring Complex "Shift". In: *Scientific and Industrial Potential of Siberia. Investment Projects, New Development Technologies*. International Catalogue. ZAO "Novosibirsk Biographical Center", Novosibirsk, p. 90–91 (in Russian) [Ружич В.В. Высокоточный измерительный комплекс «Сдвиг» // Научный и промышленный потенциал Сибири. Инвестиционные проекты, новые технологии разработки: Международный каталог. Новосибирск: ЗАО «Новосибирский биографический центр», 2004. С. 90–91].

Ruzhich V.V., Psakhie S.G., Bornyakov S.A., Smekalin O.P., Shilko E.N., Chernykh E.N., Chechelnitzky V.V., Astafurov S.V., 2002. Investigation of Influence of Vibroimpulse Excitations on Regime of Displacements in Seismically Active Fault Regions. *Physical Mesomechanics* 5 (5–6), 85–96 (in Russian) [Ружич В.В., Псахье С.Г., Борняков С.А., Смекалин О.П., Шилько Е.Н., Черных Е.Н., Чечельницкий В.В., Астафуров С.В. Изучение влияния виброимпульсных воздействий на режим смещений в зонах сейсмоактивных разломов // Физическая мезомеханика. 2002. Т. 5. № 5–6. С. 85–96].

Ruzhich V.V., Psakhie S.G., Chernykh E.N., Federyaev O.V., Dimaki A.V., Tirsikh D.S., 2007. Effect of Vibropulse Action on the Intensity of Displacements in Rock Cracks. *Physical Mesomechanics* 10 (1), 19–24 (in Russian) [Ружич В.В., Псахье С.Г., Черных Е.Н., Федеряев О.В., Димаки А.В., Тирских Д.С. Влияние виброимпульсных воздействий на

активность смещений в трещинах горного массива // Физическая мезомеханика. 2007. Т. 10. № 1. С. 19–24].

Ruzhich V.V., Vakhromeev A.G., Levina E.A., Sverkunov S.A., Shilko E.V., 2020. Seismic Activity Control in Tectonic Fault Zones Using Vibrations and Deep Well Fluid Injection. *Physical Mesomechanics* 23 (3), 54–69 (in Russian) [Ружич В.В., Вахромеев А.Г., Левина Е.А., Сверкунов С.А., Шилько Е.В. Об управлении режимами сейсмической активности в сегментах тектонических разломов с применением вибрационных воздействий и закачки растворов через скважины // Физическая мезомеханика. 2020. Т. 23. № 3. С. 54–69].

Salko D.V., Bornyakov S.A., 2014. The Automated Tool System for Monitoring of Geophysical Parametres on Geodynamic Polygons. *Pribery* 6, 24–28 (in Russian) [Салко Д.В., Борняков С.А. Автоматизированная система для мониторинга геофизических параметров на геодинамических полигонах // Приборы. 2014. № 6. С. 24–28].

Sankov V.A., Lukhnev A.V., Miroshnitchenko A.I., Dobrynina A.A., Ashurkov S.V., Byzov L.M., Dembelov M.G., Calais E., Déverchère J., 2014. Contemporary Horizontal Movements and Seismicity of the South Baikal Basin (Baikal Rift System). *Izvestiya, Physics of the Solid Earth* 50, 785–794. <https://doi.org/10.1134/S106935131406007X>.

Savransky D., 2004. Lomb (Lomb-Scargle) Periodogram. *Mathlab Central*. Available from: <https://www.mathworks.com/matlabcentral/fileexchange/20004-lomb-lomb-scargle-periodogram> (Last Accessed October 15, 2021).

Scargle J.D., 1982. Studies in Astronomical Time Series Analysis. II – Statistical Aspects of Spectral Analysis of Unevenly Spaced Data. *The Astrophysical Journal* 263, 835–853. <http://dx.doi.org/10.1086/160554>.

Scargle J.D., 1989. Studies in Astronomical Time Series Analysis. III – Fourier Transforms. Autocorrelation Function and Cross-Correlation Functions of Unevenly Spaced Data. *The Astrophysical Journal* 343, 874–887. <http://dx.doi.org/10.1086/167757>.

Seminsky K.Zh., Bornyakov S.A., Dobrynina A.A., Radziminovich N.A., Rasskazov S.V., Sankov V.A., Mialle P., Bobrov A.A. et al., 2021. The Bystrinskoe Earthquake in the Southern Baikal Region (21 September, 2020, Mw=5.4): Main Parameters, Precursors, and Accompanying Effects. *Russian Geology and Geophysics* 62 (5), 589–603. <https://doi.org/10.2113/RGG20204296>.

Sun W.F., Peng Z., Lin C.H., Chao K., 2015. Detecting Deep Tectonic Tremor in Taiwan with a Dense Array. *Bulletin of the Seismological Society of America* 105 (3), 1349–1358. <https://doi.org/10.1785/0120140258>.

Timofeev V.Yu., 2004. Tidal and Slow Deformations of the Earth's Crust in Southern Siberia According to Experimental Data. Brief PhD Thesis (Doctor of Physics and Mathematics). Novosibirsk, 36 p. (in Russian) [Тимофеев В.Ю. Приливные и медленные деформации земной коры юга Сибири по экспериментальным данным: Автореф. дис. ... докт. физ.-мат. наук. Новосибирск, 2004. 36 с.].

Timofeev V.Yu., Sarycheva Yu.K., Panin S.F., Anisimova L.V., Gridnev D.G., Masalskii O.K., 1994. Investigation of Earth

Surface Tilts and Strains in the Baikal Rift Zone (Talaya Station). *Russian Geology and Geophysics* 35 (3), 101–110.

Velde B., Dubois J., Touchard G., Badri A., 1990. Fractal Analysis of Fractures in Rocks: The Cantor's Dust Method. *Tectonophysics* 179 (3–4), 345–352. [https://doi.org/10.1016/0040-1951\(90\)90300-W](https://doi.org/10.1016/0040-1951(90)90300-W).

Vstovsky G.V., 2006. Factual Revelation of Correlation Lengths Hierarchy in Micro- and Nanostructures by Scanning Probe Microscopy Data. *Materials Science* 12 (3), 262–270.

Vstovsky G.V., 2008. Identification of Spatial and Temporal Hierarchical Structures in Complex Systems. In: R.M. Yulmetiev, A.V. Mokshin, S.A. Demin, M.Kh. Salakhov (Eds), *Fluctuations and Noises in Complex Systems of Animate and Inanimate Nature*. Shkola, Kazan, p. 441–454 (in Russian) [Встовский Г.В. Выявление пространственных и временных иерархических структур в сложных системах // Флуктуации и шумы в сложных системах живой

и неживой природы / Ред. Р.М. Юльметьев, А.В. Мокшин, С.А. Дёмин, М.Х. Салахов. Казань: Школа, 2008. С. 441–454].

Vstovsky G.V., Bornyakov S.A., 2010. First Experiences of Seismodeformation Monitoring of Baikal Rift Zone (by the Example of South-Baikal Earthquake of August 27, 2008). *Natural Hazards and Earth System Sciences* 10 (4), 667–672. <https://doi.org/10.5194/nhess-10-667-2010>.

Zhuo Y.-Q., Guo Y., Bornyakov S.A., 2019. Laboratory Observations of Repeated Interactions between Ruptures and the Fault Bend Prior to the Overall Stick-Slip Instability Based on Digital Image Correlation Method. *Applied Sciences* 9 (5), 933. <https://doi.org/10.3390/app9050933>.

Zubarev D.N., Morozov V.G., Repke G., 2002. *Statistical Mechanics of Nonequilibrium Processes*. Vol. 1. Fizmatlit, Moscow, 432 p. (in Russian) [Зубарев Д.Н., Морозов В.Г., Рёпке Г. Статистическая механика неравновесных процессов. М.: Физматлит, 2002. Т. 1. 432 с.].